Habitat suitability modelling of five Mediterranean gorgonian species

Sylvain Blouet, Lorenzo Bramanti, Katell Guizien

Habitat suitability modelling of five Mediterranean gorgonian species

Sylvain Blouet[1,2], Lorenzo Bramanti[1], Katell Guizien[1]

[1] CNRS-Sorbonne Université, Laboratoire d'Ecogéochimie des Environnements Benthiques, LECOB, Observatoire Océanologique de Banyuls Sur Mer, 66650 Banyuls sur Mer, France.

[2] Ville d'Agde, Aire marine protégée de la côte agathoise, 34300 Agde, France.

Abstract

Engineer species, such as gorgonians, provide several ecosystem services and play a significant role in the maintenance of biodiversity, which is why it is important to identify optimal strategies for their conservation. We aimed to test an ecological niche modelling approach in the marine shallow environment and identify the ecological niche of various species of gorgonians in order to lay the scientific foundation for future conservation actions. We analyzed a unique dataset of spatialized inventories on a regular grid (< 800 m) along 450 km of coastline of five gorgonian species commonly found in the Mediterranean shallow habitats (10-50 m deep). We replicated data collection in 2013 and 2020. Fourteen environmental predictors derived from the most advanced geomorphological and hydrological data were tested to assess the ecological niche of the five species using maximum entropy (MaxENT). We tested the sensitivity of the model fit to sampling bias by reducing the number of occurrences and their geographic extent. Our results showed that there was a difference in the spatial distribution of the five gorgonian species in the Gulf of Lion: *Eunicella singularis* and *Leptogorgia sarmentosa* were widely distributed while the occurrence of *Paramuricea clavata*, *Corallium rubrum* and *Eunicella cavolini* was limited. The model confirmed that depth, rugosity, slope, sea surface temperature, current and turbidity can be significant drivers for gorgonians

distribution, but in different associations, enabling one to differentiate the niche of four of the five species. Moreover, the model did not always identify the species specific drivers suggested in previous studies. Despite the model identifying a similar niche for *E. singularis* and *E. cavolini* (based on the environmental predictors tested), the two species, in fact, displayed very different spatial distributions in the area. For all the species, except *E. cavolini*, the predicted suitable habitat distribution from our model matched the observed spatial distribution. The reduction of the number of presence observations did not alter the quality of the ecological niche models as long as the observation points were spread over the entire variability range of predictors. The latter can be achieved by only including presence observations from highly protected zones of the marine protected areas of the region. Our results provide a greater understanding of the factors shaping the distribution of five gorgonian species commonly found in Mediterranean shallow areas. This is an essential step in the development of spatial planning for marine biodiversity conservation aimed at these key engineering species and their resilience to climate change.

Key words: GORGONIANS, MAXENT, MPA, DISTRIBUTION, HABITAT SUITABILITY.

Introduction

The maintenance of the ecosystem services provided by the ocean that contribute to human welfare is one of the 17 sustainable development goals identified by the IUCN for the next decade (www.iucn.org). Such an objective is encompassed in the Marine Spatial Planning framework which aims to take into account the interactions between different human activities at sea, including biodiversity protection (DIRECTIVE 2014/89/UE). One step in marine spatial planning is mapping the ocean biodiversity and the ecosystem services they deliver, together with understanding how they function, in order to be able to forecast their evolution under different development scenarios (Bailey, 2010).

During the last 20 years, several scientific programs focused on obtaining spatial information on marine habitats and the distribution range of marine species in order to begin implementing marine spatial planning. Marine species inventories, however, have generally been restricted to a limited number of locations, often in Marine Protected Areas (MPAs), although recent citizen science projects attempted to expand this spatial scale (Lorenzo et al., 2011; Ponti et al., 2019). Ecological niche modelling that requires a limited number of observations is a powerful complementary tool which refines species habitat mapping and anticipates its dynamics in the face of global changes. Ecological niche modelling currently relies on correlative approaches which are based on the assumption that the sustainable environment of a species controls its range and allows one to project species distribution range in the geographical space using environmental predictors (Sillero et al., 2021). Among the ecological niche models (ENMs), the machine learning model MaxENT - based on the principle of maximum entropy (MaxENT; Phillips et al., 2006) - only uses presence data, outperforming alternative statistical models such as GLMs that require presence-absence data, and therefore an extended dataset (Elith et al., 2006). Moreover, only using presence data avoids the assumption that the absence of a species means habitat unsuitability, when in fact it could be the result of either disturbance or ineffective dispersal (Jarnevich et al., 2015). The quality of the occurrence datasets is essential to establish an accurate model. The most commonly reported sampling biases are geographic biases - such as partial distributions and environmental biases - leading to either unreliable results or to niche estimates with underrepresented subsets of the population environmental space (Sillero et al., 2021). The pressures on the habitats can also establish a bias in the assessment of the model. Indeed, the absence of a species can result from anthropogenic pressures irrespective of the characteristics of the habitat to support this species, those being generally disregarded in niche modelling studies. Highly protected zones within MPAs might therefore be preferred locations for presence observations in order to limit confusion between predictors of ecological niche and habitats degraded by anthropogenic pressures. In the present study, we aimed to develop an ecological niche model for the most common NW Mediterranean

gorgonian species using an extensive dataset of presence and absence observations covering a wide range of environmental conditions in the NW Mediterranean Sea, including MPAs.

Gorgonians (Alcyonacea) are among the most emblematic species of the Mediterranean Sea, playing an essential role in shaping and structuring the biological diversity on the rocky temperate marine habitats (Gili & Coma, 1998; Bo et al., 2017). A high density of gorgonians visually forms underwater forests (animal forests, *sensu* Rossi et al., 2017) which increase the biodiversity and the biomass of the rocky bottom fauna inside their canopies (Ballesteros, 2006; Rossi et al., 2017). Dense canopies can reduce the impact of mucilaginous algae on understory communities, by trapping them in the upper part of their three-dimensional structures (Piazzi et al., 2018), which also limits the presence of invasive alien species (Ponti et al., 2019). The underwater landscape formed by gorgonian forests attracts scuba divers, providing significant benefits to the coastal economy (Ballesteros, 2006; Bramanti et al., 2011). Most gorgonians have a pluri-decadal life-span with slow population dynamics, slow growths and low recruitment rates. As a result, they are less resilient to frequent disturbances compared to other species (Linares et al., 2008; Garrabou et al., 2001; Sini et al., 2015; Bo et al., 2017). The conservation of gorgonians is thus a major challenge for the maintenance of the biodiversity they shelter and the economic benefits they provide. In the Mediterranean Sea, 20 species of gorgonians have been identified, two of which are endemic (*Paramuricea macrospina* and *Spinimuricea klavereni*). At international level, four species are classified by the International Union for Conservation of Nature (IUCN) as Critically Endangered (*Isidella elongata*), Endangered (*Corallium rubrum*) and Vulnerable (*Ellisella paraplexauroides* and *Paramuricea clavata*) and only two (*Ellisella paraplexauroides* and *Corallium rubrum*) are included in a regional legal framework (protocol SPA/BD, Berne Convention and GFCM recommendation). At national level, among the 24 countries and territories bordering the Mediterranean, 13 implemented specific national laws for the protection of gorgonians but they only protect one species (*C. rubrum)*, with the exception of

Montenegro and Croatia whose national laws also protect *Eunicella cavolini*, *Eunicella stricta* and *Eunicella verrucosa* (Bo et al., 2017).

Among the Mediterranean gorgonian species, five are common in the rocky communities of shallow (0-50 m) coastal waters (Weinberg, 1979a): *Eunicella singularis* (Esper, 1791), *Leptogorgia sarmentosa* (Esper, 1789), *Eunicella cavolini* (Koch, 1887), *Paramuricea clavata* (Risso, 1826) and *Corallium rubrum* (Linnaeus, 1758). The five species have a wide Mediterranean distribution despite the fact that they have been mainly studied in the northwestern area (Charbonnier et al., 1984; Cocito et al., 2002; Gori et al., 2011; Bo et al., 2012 for deep observations but see Di Camillo et al., 2018; Sini et al., 2015). Those five species are strictly associated with hard substrates, with the exception of *L. sarmentosa*.

P. clavata, *C. rubrum* and *E. cavolini* have a wide bathymetric distribution from -10 m to >-100 m (Bo et al., 2012; Carugati et al., 2022). In the shallow area, the species have been associated with different geomorphological preferences. *C. rubrum* is mainly found in overhangs or in caves (Cau et al., 2016). *P. clavata* and *E. cavolini* are reported to dwell in steep rocky coralligenous bottoms, such as drop-offs, and they are often found together (Carugati et al., 2021). *L. sarmentosa* is found in the detritic-muddy benthic community, characterized by boulders and organic matter (Carpine & Grasshoff, 1975; Mistri & Ceccherelli, 1993). *E. singularis*, which is the only one of the five species harbouring zooxanthellae (Forcioli et al., 2011), is found on well-lit horizontal and sub-horizontal rocky bottoms (Gori et al., 2011; Weinberg & Weinberg, 1979). *E. singularis* and *L. sarmentosa* can be associated with gently sloping rocky bottoms as well (Gori et al., 2011). The five species release planula larvae with dispersal distances of tens of kilometers (Guizien et al., 2020).

In this study, we analyzed the spatial distribution of *E. singularis*, *L. sarmentosa*, *E. cavolini*, *P. clavata* and *C. rubrum* in their shallow bathymetric range (10-50 m) over a wide geographic area (450 km²), along the French Mediterranean coasts (Toulon to Cerbère), using spatialized inventories performed on a regular grid (< 800m) covering the rocky habitat. The ecological niche and distribution area of

suitable habitats were modelled with MaxENT software to identify the main environmental predictors that influence the spatial distribution of the five species. We also assessed whether a sampling restricted to the 5 highly protected zones of the MPAs within the study area (which can be considered free from the main anthropogenic pressures impacting the gorgonians such as anchoring, nets, scuba diving, *etc*.) would affect model predictions. We also tested the sensitivity of the model fit to a reduced number of occurrences and their geographic position. As a result, we were able to provide indications on sampling design for future studies aimed at predicting the range of gorgonian suitable habitats.

Materials and methods

Study area

The study area is extended along 450 km of the French Mediterranean coastline, from Toulon to Cerbère, and from the coast down to the 50 m isobath. Along this coastline, the benthic habitat mainly consists of soft bottom with a few small patches of rocky habitat of less than 590 000 km². A set of eight sites (National Park of Port Cros: PNPC, Parc Marin de la Côte Bleue: PMCB, Aigues-Mortes: AGM, Aresquiers: ARES, Agde: AGD, Valras: VLR, Leucate: LEU, Côte Vermeille: CVM; Figure 1) within this fragmented rocky habitat were investigated to assess the niche preferences of the five erect octorallia: *Eunicella singularis*, *Eunicella cavolini*, *Paramuricea clavata*, *Leptogorgia sarmentosa* and *Corallium rubrum*. Of the eight sites, five include a high protection zone (according to the classification of Horta e Costa et al., 2016: Fully protected) with different surface areas (PNPC: 1232 ha, AGM:100 ha; AGD: 310 ha, CVM: 69 ha; PMCB: 289 ha) (Figure S1).

Data collection

Species presence

The population density of the five species was assessed between 2013 and 2021 in 696 evenly spaced geo-referenced locations covering the hard bottom habitat in all sites except in PNPC where locations

were selected based on the known presence of the species *P. clavata* (Guizien et al., 2022; https://cardobs.mnhn.fr/; Figure 1 and Figure S1). The spacing between sampling points varied from 100 m to 800 m, depending on the bathymetrical steepness of each zone. Using a regular grid in order to avoid the bias of preferential sampling enabled us to estimate that no spatial auto-correlation was observed (Legendre et al., 2002; Merckx et al., 2011). For the five species, a strong nugget effect (Carrasco, 2010) at eight meters distance was observed on empirical variograms (Figure S2). In each georeferenced location, all individuals larger than 2 cm (i.e. older than one year) were counted either by direct visual census of autonomous scuba divers or on photographs in four to nine quadrats of $1m^2$. These surface areas were larger than the minimal area of $2m^2$ established for shallow water octocorallia communities (Weinberg, 1978).

The georeferenced database of the five species presence was implemented in GIS software (© QGIS).

Habitat suitability model

The Maxent model

MaxEnt is a machine learning software recognized as the most efficient method in species distribution modelling when presence-only species records are available (Elith et al., 2006; Hernandez et al., 2006, 2008; Bargain et al., 2018). Natively, MaxEnt estimates Relative Occurrence Rate (ROR) which is defined as the probability for an observed individual to be found in a set of environmental conditions by maximising its entropy probability distribution (i.e., the most spread out or closest to the uniform, Phillips et al., 2006). Hence, MaxEnt is a niche or habitat suitability model whose predictions, although represented on a spatial grid, relate to environmental variables only, disregarding spatial locations arrangements except if geographical variables are explicitly included in the set of environmental descriptors (Elith et al., 2011) . The Maxent version 3.4.4 was used.

Setting up the MaxEnt model requires defining background data, features, regularization multipliers, sampling biases, output types, and diagnostics outputs. The quality of Maxent fits is primarily assessed by the Area Under the ROR Curve (AUC). The AUC ranges from 0 (fit worse than random) to

1 (perfect fit). Below 0.5 the prediction is not better than at random, and above 0.7 the prediction is reliable (Zweig & Campbell, 1993).

Background data encompass the definition of a set of grid cells where presence/absence of the species is unknown (a prior with uniform species prevalence is defined) but the type of environmental predictors and their values are known (hereinafter called Maxent grid). As probability distribution of environmental predictors in the Maxent grid is compared to probability distribution of environmental predictors in presence locations in order to build response curves, Maxent grid actually defines the range of environmental conditions on which features will be fitted in order to maximize the species entropy probability distribution, resulting in different features and MaxEnt predictions according to background extent.

Sampling bias was reduced by using a background grid targeting the hard bottom habitat where the five octocoral species exclusively dwell. In the eight sites, a large part of the hard bottom habitat was gridded with a set of 468 georeferenced 100m x 100m cells, according to availability of environmental predictors data (Figure S1). Among the recorded presence for each species in the eight sites, however, only a subset was found in the Maxent grid. *C. rubrum* was present in 16 grid cells, *P. Clavata* in 20 grid cells, *E. cavolini* in 32 grid cells, *L. Sarmentosa* in 63 grid cells and *E. singularis* in 264 grid cells. Data on marine habitats were retrieved from CARTHAM website (https://geo.data.gouv.fr). The implementation of habitats and masks was carried out in © QGIS software.

The environmental predictors were selected within all available geomorphological and hydrological potential predictors, to which were added latitude and longitude as explicit predictors in some modelling test**.** Geomorphological predictors were calculated from raw bathymetrical dataset that combined three-dimensional point seedlings from Airborne Laser Imaging Detection and Ranging

System (LIDAR) for water depth less than 15 m (LITTO3D, www.diffusion.shom.fr) and multibeam echosounder for water depth larger than 15 m, except in PNPC where LIDAR data extended down to 40m water depth. LIDAR data was collected between 2014-2015, except in the CVM zone where it was obtained in 2011. Multibeam echosounder data was assembled from multiple collection periods between 2005 and 2018 and from different operators (Seaview for AGM, ARES and VLR; CEFREM for CVM; Semantic for AGD; Copethec and Mesuris for PMCB). Density of LIDAR data decreased from 10 points.m² to 0.1 points. m² when water depth increased. Density of multibeam echosounder data decreased from 25 points.m² to 4 points. m².

Seven geomorphological metrics commonly used for habitat predictive modelling were computed for each cell of the Maxent grid. These seven metrics describing the seafloor topography were: bottom depth (unit: m), slope (unit: angle degrees), roughness (unit: m), rugosity (no unit), terrain ruggedness index (TRI; unit: m), eastness (no unit) and northness (no unit) orientation (Wilson et al., 2007). These metrics were calculated using all raw bathymetrical data within a 20 m x 20 m slab located in the center of each cell of the Maxent grid.

- Local bottom depth was the average of bathymetric data within the slab.
- A local digital terrain model (DTM) was defined by interpolating all bathymetrical data within the slab with a bivariate quadratic equation (1) (Evans, 1980):

$$Z = aX^2 + bY^2 + c\,XY + dX + e\,Y + f \quad (1)$$

with Z being the bottom depth deviation from the mean bottom depth and X,Y the cartesian distance to the center of the Maxent grid cell.

- Slope was defined as the average slope of the local DTM:

$$S = \arctan\left(\sqrt{\left(d^2 + e^2\right)}\right)$$

- Roughness was defined as the difference between the maximum and minimum depth in the slab.

- Rugosity was defined as the ratio between the surface of the local DTM and the slab surface. By definition, rugosity is larger or equal to 1.
- Terrain ruggedness index was defined as the average of absolute deviation of the local DTM with respect to the mean depth.
- Eastness and northness orientation were defined as the sinus and cosinus of the DTM aspect, the latter being defined as:

$$\text{Aspect} = \text{atan}(d/e)$$

Hydrological predictors included turbidity and temperature which were measured at the sea surface by satellite imaging (Aquamodis - level-3 global browser : https://oceancolor.gsfc.nasa.gov/l3/) and simulated current speed at the sea surface by a coastal ocean circulation model (Briton et al., 2018). Satellite observations came from the Moderate Resolution Imaging Spectroradiometer (MODIS) on board the AQUA satellite. Data was acquired in 36 spectral bands at three resolutions (250, 500 and 1000 m) and covered all the globe in one to two days. Sea Surface Temperature (SST, unit: °C, 4 µ night time) and turbidity (unit: m-1, Diffuse attenuation coefficient at 490 nm) monthly averages at 4 km spatial resolution were extracted between 2003 and 2018 for Turbidity and 2006 and 2018 for SST over the extent of the Maxent grid. For each variable (SST, Turbidity), the pluri-annual mean was calculated and interpolated at the Maxent grid resolution of 100 m. Although Chlorophyll a concentration is one of the MODIS products (Chla, unit: mg.m-3, OCx Algorithm), it was not considered because data was missing in the PMCB site. However, Chlorophyll a concentration significantly correlated with turbidity in all other sites (Spearman correlation determination $R^2 = 0.68$, $p < 10e\text{-}4$). The coastal ocean circulation simulated data in the NW Mediterranean sea came from hourly output of a SYMPHONIE 2015 which ran from January 2010 to December 2012 (Briton et al. 2018). The simulation was performed on a 680 x 710 curvilinear horizontal grid and 29 vertical levels of generalised sigma-coordinates covering an area between 3°E and 8°E, 40.5°N and 44°N and from 3m to 3000m water depth forced by the three-hourly regional downscaled climate simulations

NM12-FREE (Hamon et al., 2016). Monthly statistics (Umin = Q10 and Umax = Q90, unit: m.s-1) of flow speed hourly values at the sea surface were computed. Those statistics were then interpolated in each cell of the Maxent grid. Because flow speed predictions on the rocky habitat near the coast were limited by the model vertical resolution, the simulation grid did not cover the entire rocky habitat and a zero flow value was assumed at the coast while interpolating.

Uncorrelated predictors were selected within the 13 environmental predictors, together with the geographical predictors, to avoid confusion in predictor identification in Maxent as a result of predictor redundancy. Correlations between all possible pairs of predictors were calculated using Spearman's determination coefficient (Figure S3), together with Principal Components Analysis (Figure S4). When the determination coefficient of a pair of predictors exceeded 0.7, and their first and second components on the PCA plot were close, one of the two predictors was discarded (Sillero et al., 2021) Figure S4). Among the 13 potential predictors, 10 were not correlated: five geomorphological predictors (Depth, Slope, Rugosity, Eastness and Northness), three hydrological predictors (Umax, SST and Turbidity) and the two geographical predictors (Latitude and Longitude). For each of these 10 predictors, their range was assessed across the five species presence location sets, across the entire Maxent grid. The Maxent grid was restricted to any of the eight sites and sampling bias was assessed. All data processing was performed using in-house Matlab© routines.

Features and regularization

Various feature classes can be combined in Maxent to build response curves from environmental variables. Theoretically, a niche model is expected to be unimodal, pointing at species optimum, which will be best represented by quadratic features. Sometimes the niche range, however, might be truncated in the presence observations. In this situation, linear or hinge features will be more appropriate (Merow et al., 2013). Multiplying feature class possibilities may lead to confusion because complex features created by MaxEnt are often highly correlated. From a statistical

perspective, when MaxEnt is used to infer environmental drivers of species distribution, feature classes should be selected with parsimony. From a machine-learning perspective, testing as many feature classes as possible will increase the predictive accuracy of the presences. In this study, we adopted an in-between perspective, selecting the default "auto-features" mode of Maxent. This mode increases the tested feature classes to the number of presence observations with all feature classes for more than 80 presence observations (Phillips & Dudık, 2008). This mode enabled Maxent to accommodate the different number of presence observations, which varied from 39 for *C. rubrum* to 479 for *E. singularis*. Regularization dampens predictors coefficients when predictors variance is high at the presence locations. Regularization multiplier was varied from 0.1 to 5 and the AUC of model fit varied by less than 1%. Hence, it was set to its default value of 1.

Output type

The ROR is the relative probability that a cell is contained in a collection of presence samples, assuming individuals have been randomly sampled in the environmental space. A logistic transformation of ROR enables one to predict the probability of presence only, assuming the prevalence that is the probability of presence in the suitable habitat is 50% (Phillips & Dudık, 2008). Due to the difficulty of checking this assumption, the safer interpretation of MaxEnt predictions was using ROR as a habitat suitability index (Merow et al., 2013). As an alternative, the cloglog value corresponding to a ROR value of r is 1-exp(-c·r) has been proposed in order to estimate the probability of presence (Anderson et al., 2017). In the present study, however, model fit was not sensitive to the species prevalence value in the background grid. The latter varied from 20 to 80% and resulted in average AUC (Area Under the Curve) variation of 0.6%. Therefore, prevalence was kept to its default value of 50% and the cloglog output type was selected.

Diagnostics of model fitting

Model best fit was the average of five replicated probability maps fitted using all predictors under the cross-validate option. For each replicated fit, the presence data was partitioned randomly (random seed option) into a training dataset used to fit the model (75% of presence data) and a testing dataset (25% of presence data). AUC on the training datasets and testing datasets and the relative contribution of each predictor to the replicated fit were calculated to assess the quality of the fit.

The contribution of each predictor in defining each of the five replicated fits was ranked using a jackknife cross-validation procedure (Phillips et al., 2006). To do so, for each of the five presence data partitions, replicated fits were constructed using either a predictor on its own or all predictors except the one in question. Gains and losses of AUC compared to the AUC with all variables were calculated with and without each predictor, respectively.

Another ranking of the contribution of each predictor to a model was performed using a permutation procedure. For each predictor in turn, the values of that predictor in the training presence and background data were randomly permuted. The model was then re-evaluated on the permuted data, and the resulting drop in training AUC indicated that the model depended heavily on that predictor. Values were normalized to give percentages.

Predictor response curves showed how the predicted probability of presence varied with the predictor, holding all other environmental variables at their mean sample value or using only the corresponding variable.

Sensitivity of model fitting to potential sampling bias when reducing presence number and their geographical extent

Sampling bias can appear when some environmental conditions are preferentially sampled without respecting the proportion of their availability (Merow et al., 2013). Sampling bias can be the result of geographical or temporal preference in presence exploration or limited presence exploration. Such bias is evident for rare species whose niche is limited in space and requires intensive exploration to

be observed. For more widely distributed species, sampling bias is less evident. Among the five gorgonian species, we selected the two species with highest occurence: *E. singularis* (264 presence data) and *L. sarmentosa* (63 presence data), and assessed the sensitivity of the AUC when decreasing the number of presence data in the training dataset (while still keeping the full presence dataset for testing). To do so, we followed two procedures. In the first procedure, the model was fitted using three training datasets, gradually reducing the number of presence data to an evenly distributed selection of 50%, 20% and 10% of the initial training dataset. In the second procedure, the model was fitted using a reduced number of presence data in the training datasets, corresponding to geographical restrictions to six sites for *E. singularis* (CVM, AGD, ARES, AGM, PMCB and PNPC) and two sites for *L. sarmentosa* (CVM and AGD). For both species, a training dataset including only presence recorded within MPAs was tested as well. Finally, sampling bias was also tested by testing if adding the geographical coordinates as predictors altered the model fitting.

Model performance assessment

Performance of two models, one using the full presence dataset and the other only using the presence observed in MPAs, were compared. Model performance was assessed by contrasting the habitat suitability predictions with observed presences and absences for each of the five species.

For each species, regional habitat suitability maps were built after binarizing the mean of the five replicated probability maps. This was done by applying a threshold probability above which the habitat was considered as suitable and below which it was considered as unsuitable. Due to varying prevalence among the five species, the threshold probability was not set to a fixed value but instead was determined using one of the 11 possible thresholding procedures advised in Maxent (Anderson et al., 2017). Deciding which threshold to use is a major consideration when minimizing false positives and false negatives. his choice, however, is often arbitrary in studies (Liu et al., 2005). Among these threshold procedures, the 10percentile_training threshold (maximum error rate of 10% on the presence points of the learning data) was arbitrarily selected because it displayed the highest

threshold values when compared to other thresholding procedures, resulting in the less extended and hence more conservative habitat suitability maps (Figure S5).

A frequency contingency table was built that compared observed presence and absence with predicted ones in the 468 grid cells. Accuracy (the proportion of correctly predicted presence and absence), sensitivity (the proportion of correctly predicted presences), specificity (the proportion of correctly predicted absences) and true skill statistic (TSS, sensitivity + specifity -1) were calculated. The latter scores the model performance between -1 and 1 with 0 indicating a random model and +1 the perfect agreement. This approach was favoured and used instead of the kappa indicator (Cohen 1960) which intrinsically depends on the prevalence (Allouche et al., 2006). The significant deviation from a random contingency table was tested with a chi2 statistics (Pearson, 2007).

Results

Species presence observations and sampling bias assessment

In the study area, the observed spatial distribution varied among the five species. Some species were distributed in a limited number of clustered locations: *C. rubrum* with 39 presences in only two sites (CVM and PMBC, Figure 2), *P. clavata* with 61 presences in three sites (CVM, PMBC and PNPC, Figure 2) and *E. cavolini* with 87 presences distributed in three sites (PNPC, PMCB and ARES, Figure 2).

L. sarmentosa was detected everywhere except in PNPC and AGM (Figure 2). Finally, *E. singularis* was the most widespread species with 479 presences, distributed in all eight sites (Figure 2). The most frequent association was observed between *E. singularis* and *L. sarmentosa* (17.9%).

Boxplots that represented the environmental predictors range, showed marked differences among the eight sites forming the background seascape (Figure 3). Depth range was doubled in four out of the eight sites, extending down to 40 meters depth (CVM, AGD, PMCB and PNPC, Figure 3). Larger slope and rugosity were found in two (PNPC and CVM) out of the eight sites, while seabed

orientation (eastness and northness) displayed a similar range of variability in all eight sites (Figure 3). Higher sea surface temperature (SST, Figure 3) and lower turbidity characterised three out of the eight sites (CVM, PMCB and PNPC, Figure 3). Finally, larger maximum flow speed at the seabed was frequently found in five out of the eight sites (LEU, VLR, AGD, ARES, AGM, Figure 3).

Boxplots that represented environmental predictors range at species presence locations, indicated some differences between species as well. Maximum flow speed at the seabed was consistently higher at presence locations of *C. rubrum* than of any other species (Figure 3). Sea surface temperature was consistently lower at presence locations of *C. rubrum*, *E. singularis* and *L. sarmentosa* than of *P. clavata* and *E. cavolini* (Figure 3). Turbidity was higher at presence locations of *E. singularis* and *L. sarmentosa*, while slope was slightly higher at presence locations of *P. clavata* than at other species presence locations (Figure 3).

Environmental predictors contribution to habitat suitability prediction

Different environmental predictors contributed to the Maxent model best fit of each gorgonian species in (when only using the presence locations found in the background data, Figure 2).

For *C. rubrum*, turbidity and maximum flow speed at the seabed (Umax) contributed more than 90% to the suitable habitat prediction (both in percent contribution and permutation percentage, Table 1). Response curves for these two predictors indicated species preference for current speeds greater than 0.23 m/s and turbidity lower than 508.8 m^{-1} (Figure S7), suggesting that the ecological niche of *C. rubrum* extends beyond the variation range of those predictors within the background grid of the study. Turbidity was the predictor that, when absent, most decreased the AUC in the model, while maximum flow speed at the seabed contributed the most to the AUC in stand-alone mode, followed by depth and rugosity (Jacknife's test, Figure S6).

For *P. clavata*, depth and rugosity combined contributed to more than 60% of the suitable habitat prediction (both in percent contribution and permutation percentage, Table 1). Slope had the third greatest contribution when it came to suitable habitat prediction, yielding about 15%. Response curves of the three predictors indicated species preference for water depth greater than 21 m, rugosity greater than 1 and slope greater than 3.3% (Figure S8). All response curves displayed a plateau when they reached high values, suggesting the species can distribute beyond 50 m water depth. Depth was the predictor that most decreased the AUC when it was not included in the model and contributed the most to the AUC in stand-alone mode (Jacknife's test, Figure S6).

For *E. cavolini*, rugosity, sea surface temperature and depth combined contributed more than 90% to the suitable habitat prediction (both in percent contribution and permutation percentage, Table 1). Response curves indicated that *E. cavolini* had a preference for sea surface temperature above 16°C, water depth greater than 12 m and bed rugosity larger than 1 (Figure S9). None of these predictors displayed a niche-like optimal range of values. Rugosity and depth were the variables that most reduced the AUC when removed from the model, while sea surface temperature contributed the most to the AUC in stand-alone mode (Jacknife's test, Figure S6).

For *E. singularis*, rugosity, sea surface temperature, depth and rugosity when combined, contributed to about 80% of the suitable habitat prediction (both in percent contribution and permutation percentage, Table 1). Response curves indicated that *E. singularis* had a preference for sea surface temperature ranging from 15.8 and 17.5°C, water depth ranging from 4 to 40 m, with a characteristic niche-like optimal range of values and rugosity larger than 1 (Figure S10). Sea surface temperature was the variable that most decreased the AUC when removed from the model and contributed the most to the AUC in stand-alone mode (Jacknife's test, Figure S6).

For *L. sarmentosa*, depth, rugosity, sea surface temperature and turbidity when combined, contributed more than 90% to the suitable habitat prediction (both in percent contribution and

permutation percentage, Table 1). Response curves indicated that a preferential habitat for *L. sarmentosa* would be in areas with a temperature below 17.1°c, and in terrain with rugosity between 1 and 5, and with a turbidity of between 215.7 and 603.4 m^{-1} (Figure S11).

Sea surface temperature and depth were the two predictors that most reduced the AUC when they were absent from the model and they contributed the most to the AUC in stand-alone mode (Jacknife's test, Figure S6).

Overall, sea surface temperature was identified as primary environmental predictors for three species and turbidity was the primary predictor for two species out of five. Among geomorphological predictors, rugosity and depth contributed to suitable habitat modelling, while no orientation predictors did. Despite rugosity being a significant predictor for all species, rugosity response curves did not indicate much discrimination between the species, when any rugosity larger than 1 was favourable. Minimum flow speed did not contribute to the suitable habitat modelling of any of the five gorgonians.

Model performance and assessment of the predictions

Average AUC varied from 0.799 to 0.971 across the five species, indicating good to very good fit when learning and testing against replicated random partitions of the presence dataset (Table 1). Maps of suitable habitats that were obtained after applying a thresholding occurrence probability to model best fit, demonstrated correct predictions when compared to both presence and absence observations for all species, with accuracy ranging from 66% for *L. sarmentosa to 92% f*or *P. clavata*. In all species, true skill statistics (TSS) differed significantly from a random contingency table. However, true skill statistics ranked the model performance differently to the AUC across species. While prediction for *E. singularis* displayed the lowest AUC (0.799), it displayed the highest TSS (0.48), resulting from the highest sensitivity (0.72). Conversely, the AUC prediction for *E. cavolini* was high (0.901) but TSS was the lowest (TSS: 0.17), due to a low sensitivity (error in predicted presence)

of 0.18 (Table 2). Predicted suitable habitat was larger than the actually observed one when looking at presence and absence data for all species, except for *E. singularis*. This latter species was found in about 5% of cells classified as unsuitable habitat. The predicted suitable habitat was 20% larger than the observed one on average across all species, with higher values for *L. sarmentosa* (30%) and for *E. cavolini* (27%).

Moreover, prediction errors differed across species. For two species, predictions suggested the suitable habitat would extend more than the observed one within sites where the species presence had been recorded (*P. clavata*, *L. sarmentosa*). For two other species, suitable habitat was predicted in sites where the species presence was not detected (*C. rubrum* and *E. cavolini*).

Assessing the influence of the number and location of presence observations used for model training on model fit goodness

Sensitivity of model AUC to the number and location of presence observations used for model training was carried out on *E. singularis* and *L. sarmentosa* because these species have the widest spatial coverage and the greatest number of presence.

For *E. singularis* and *L. sarmentosa*, model AUC remained within the range of variation of the five replicated model AUCs when the training dataset was reduced by 90% and 80%, respectively, as long as the presence observations of the training dataset were spread in all sites where the species was observed (Figure 4). In contrast, model AUC decreased sharply when the number of presence observations was reduced by the same amount but restricted to a single site only (Figure 4). When the number of presence observations was restricted to the highly protected zones of the area, model AUC decreased to 0.7 for *E. singularis* and 0.85 for *L. sarmentosa*. This decrease was, however, less than if the same number of presences had been taken from a single site, although slightly more than if it was evenly distributed in all eight sites. Model AUC, when the number of presence observations was restricted to the highly protected zones of the area, remained high as well or even increased for *C. rubrum*, *P. clavata* and *E. cavolini*, with accuracy ranging from 0.66 to 0.92 (Table 2).

Adding latitude and longitude to the environmental predictors improved the average test AUC for all species except for *C. rubrum*. Suitable habitat maps, however, remained unchanged or changed slightly when adding longitude and latitude for *C.rubrum*, *P.clavata* and *E. singularis*. For *L. sarmentosa*, adding geographical predictors altered predicted distributions, resulting in the loss of two sites where the species has been observed (PMCB and ARES, Figure S12).

In contrast, the suitable habitat map for *E. cavolini* changed considerably, with an area that reduced from 12.56% to 7.4%. The suitable habitat area was removed in CVM and partially reduced in AGD with improvement of accuracy and TSS (to 0.96 and 0.62 respectively, Figure 2a).

Discussion

The observations between 10 and 50m water depth across eight rocky sites spanning 450 kms along the Gulf of Lion (NW Mediterranean sea) confirmed that between 2013 and 2020 the hierarchy in the occurrence of the five gorgonian species was similar to the one previously reported in the same area (Weinberg, 1979a; Weinberg & Weinberg, 1979; Linares et al., 2008; Gori et al., 2011). *E. singularis* was the most abundant of the gorgonian species, with a wide continuous spatial distribution. *L. sarmentosa* was the second most abundant gorgonian species, with scattered distribution. *P. Clavata* and *C. rubrum* displayed highly patchy distributions and their presence was observed in three rocky sites only. *E. cavolini* was the least abundant species, with marginal presence in a few spots in three rocky sites. Occasional associations between the five gorgonian species were observed but were not frequent, similar to what was previously reported for the shallow area (Gori et al., 2011).

Geomorphological (Depth, Slope, Rugosity, Eastness and Northness) and hydrological (Umax, SST and Turbidity) predictors enabled an accurate projection of habitat suitability for all gorgonian species, except for *E. cavolini*, for which the predicted suitable habitat was larger than what was observed, and was considerably reduced when explicitly adding a geographical predictor. For the other four gorgonian species, we showed that presence observations used in the training dataset could be

reduced to 14 without altering predicted suitable habitat, most likely due to the fact that the spatial extent of the training dataset was large enough to encompass the range of variation of predictors in the area. In the extended Gulf of Lion, a wide variability range could be achieved for each predictor, with a sampling focused solely on the zones of high protection of the MPAs. The models showed that currents (> 0.23 m/s) and turbidity (< 508.8 m^{-1}) were the main predictors for *C. rubrum* , depth (> 21 m) and wall inclination (> 3.3%) for *P. clavata*, depth (4-40 m; > 16 m) and surface temperature (SST) (15.8-17.5°C; > 16°C) for *E. singularis* and *E. cavolini* and turbidity (215.7 and 603.4 m^{-1}) and rugosity (1-5) for *L. sarmentosa*.

High resolution terrain mapping that combines airborne and satellite remote sensing has been an essential data source for determining species habitats (when using predictive habitat modelling in terrestrial environments, Wilson et al., 2007). In the ocean, bottom surface variability is expected to be an essential structuring factor as well, with variations in substrate altitude including at a very small spatial scale (< 1mm) acting on colonization (Carleton & Sammarco, 1987; Nozawa, 2008; Brandl et al., 2014; Sempere-Valverde et al., 2018). At sea, however, high resolution seabed mapping is relatively new. Vessel-mounted multibeam acoustic sounders can provide terrain maps with a vertical resolution at the cm scale and horizontal resolution at the tens of cms scale but over a limited area (Dolan et al., 2008). The cost of acquiring such data has limited its implementation, which is why predictive habitat modelling studies have focused on specific environments such as canyons (Guinan et al., 2009; Bargain et al., 2018; Lo Iacono et al., 2018). The present study aims to fill a gap in predictive habitat modelling for shallow environments by leveraging recent advances in bathymetry remote sensing using airborne laser imaging, which enable mapping shallow areas along the coastline, with spatial resolution similar to that of vessel mounted acoustic sounder.

Our results showed that among geomorphological predictors, depth was significant for all species, except *C. rubrum*. Depth is a primary factor that modulates both light availability and agitation at sea

(Perez, 1961). It has long been recognised as a proxy for the niche of benthic species, to such an extent that it is used as a basis for the classification of marine benthic communities strata (Odum, 1971). In the present study, depth was identified as a major predictor for all species distribution except *C. rubrum*, but with different responses. For *P. clavata* and *E. cavolini*, model predictions suggested a preference for deeper habitats as already mentioned in the literature (Rossi, 1959; Boavida et al., 2016; Fourt et al., 2017;). By contrast, *E. singularis* and *L. sarmentosa* model predictions indicated a preference for shallow areas (between 10 and 40 m). Yet, both species have been reported beyond 50m depth (Weinberg, 1979a; Bo et al., 2012; Grinyó et al., 2016). Deep and shallow populations of *E. singularis* display different morphotypes with limited gene flow between them at local scale (Gori et al., 2012; Costantini et al., 2016). While extending the depth range of observations should improve habitat suitability delineation, species adaptation may reshape habitat suitability boundaries. For *C. rubrum*, depth was not identified as a significant predictor, despite the fact that the species preference for low light has been largely reported (Laborel, 1960; Weinberg, 1979b; Bianconi et al., 1988).

Seabed orientation is another proxy for light availability that has been used in several studies at small spatial scale (Glasby, 2000; Knott et al., 2004). However, in the present study, orientation was never indicated as a significant predictor. This was, in all likelihood, due to the fact that orientation and light availability are not correlated over a large spatial scale.

The presence of *C. rubrum* at shallow depth might, instead, be related to the smaller size of this species, compared to the other four gorgonian species, which would allow for the colonization of small crevices (Laborel, 1961; Rossi et al., 2008). In any case, despite the fact that depth is easier to measure than light, direct measurement or modelling of light intensity should be undertaken to improve the delineation of the species niche (Betti et al., 2018).

Surprisingly, rugosity, a measure of terrain irregularities which is expected to depict small crevices favourable to *C. rubrum*, was an important predictor for all species except *C. rubrum*. Rugosity estimates, in fact, vary with terrain sensing resolution (Wilson et al., 2007). In the current study, the LIDAR resolution did not enable the detection of crevices smaller than 0.1 m in which *C. rubrum* colonies are often found (True, 1970; Virgilio et al., 2006). Given the current LIDAR resolution, the maximum detectable rugosity was seven, which was sufficient to differentiate the suitable habitat of *L. sarmentosa*, which is mainly found at a moderate rugosity and that of the other three species (*P. clavata*, *E. singularis* and *E. cavolini)* which can be found on a wider range of rugosities. Slope is another parameter often assumed to explain the colonization of benthic communities, as the deposition of organic matter on flat surfaces could limit the recruitment of some benthic invertebrates (Laborel & Vacelet, 1961; Bianconi et al., 1988; Glasby, 2000). However, among the five suspension feeders of the present study, only *P. clavata* preferentially colonized substrates steeper than 3.3%. This finding is consistent with previous studies in the shallow environment (Cocito et al., 2002; Boavida et al., 2016; Ponti et al., 2019). Nevertheless, giant colonies of *P. clavata* have been observed in PMCB on deep horizontal rocks between 40 and 60m (https://theconversation.com/une-plongee-dans-les-forets-animales-formees-par-les-gorgones-en-mediterranee-176399). Just as we found with depth, by extending the number of observations, the significance of slope in shaping *P. clavata* suitable habitat could change, suggesting that the direct measurement of sedimentation would better define species suitable habitat.

Sea water turbidity remotely sensed from satellites is another predictor that can indicate sedimentation due to river inputs or to sediment resuspension by waves (Liew et al., 2009; Gohin et al., 2020). High sedimentation is sometimes considered a limiting factor for gorgonians (Bo et al., 2017). However, in our study, it was not identified as a major predictor of the suitable habitat for *P. clavata*, *E. singularis* or *E. cavolini*. An upper limit for tolerance to turbidity was only found for *C. rubrum* and *L. sarmentosa*. In addition, as suggested in previous studies, *L. sarmentosa* prefers some

minimum turbidity, unlike *C. rubrum* (Weinberg, 1979a; Mistri, 1995). *L. sarmentosa's* preference for turbid seawater would have resulted in the species adapting morphologically with higher polyp density per branch and finer branches to reduce the surface offered to sediment accumulation in turbid environmental conditions, compared to the other four gorgonian species (Cocito et al., 2002; Rossi et al., 2011). Preference for turbid environments can be expected in suspension feeders and might be related to food requirements as this predictor was positively correlated with Chlorophyll a. The diet of *L. sarmentosa* like that of *P. clavata* and to a less extent of *E. singularis* is primarily based on small zooplankton (Rossi & Rizzo, 2021), whose abundance is tightly related to the abundance of Chlorophyll a. When combining polyps density per branch with the number of preys ingested per polyp (Coma et al., 1995; Rossi & Rizzo, 2021), *L. sarmentosa* displayed a higher ingestion rate than *P. clavata* and *E. singularis*, a trait that could be related to its preference for turbid habitat.

Sedimentation can be locally reduced by strong current (Hiscock, 1983) and current has been suggested as structuring the distribution of gorgonians (Leversee, 1976; Weinberg, 1979a) and corals (White et al., 2005). According to experts, the five gorgonian species have a preference for moderate to strong current (La Riviere et al., 2021). The present study identified strong current as a structuring predictor for *C. rubrum* only. In fact, current is not commonly used as a predictor in ecological niche models and should be more systematically tested using hydrodynamical model outputs (see Bargain et al., 2018).

Just as with current, sea surface temperature is not commonly used as a predictor for *E. singularis* and for *L. sarmentosa* presence, probably due to their tolerance to environmental conditions, given that these two species can be found even inside ports, where water temperature can reach 29°C (Betti et al., 2018; S. Blouet comm pers,). However, mass mortalities in *E. singularis* and *E. cavolini* have been related to temperature anomalies during heat waves (Coma et al., 2006; Ezzat et al., 2013; Turicchia et al., 2018), as with *P. Clavata* populations which were infected by a thermo-dependent

bacterial pathogen whose virulence increased with elevated temperature (Bally & Garrabou, 2007; Garrabou et al., 2009). However, our results indicated that only the suitable habitat of *E. singularis* and *L. sarmentosa* is linked to mean annual sea surface temperature with a preference for lower values (< 17.5°C). It is worth noting that during summer periods, below 20 m depth, the water temperature can be very different from the sea surface temperature used in the present study.

In summary, identifying the suitable habitat for marine species still faces limitations and will require both increasing the number of presence observations to deeper areas and including more explicitly factors such as temperature, light, turbidity, sedimentation, chlorophyll a and current. To this end, the use of high-resolution simulations of circulation and primary production would be an invaluable tool for contemporary ecological studies, as they allow one to project the distribution of the future suitable habitat in climate change scenarios and test the deep refugia hypothesis (Bongaerts et al., 2010).

Nevertheless, despite the limitations mentioned above, model performance was high for all species except *E. cavolini*, with AUC values and accuracies indicating good predictive quality of suitability habitats (Hanley & McNeil, 1982). The good sensitivity of the models for *E. singularis* and *L. sarmentosa* with few but regularly distributed observations of presence, confirms, on the one hand, that spatial autocorrelation was avoided and that large AUC values could not be attributed to model overfitting (Radosavljevic & Anderson, 2013) and, on the other hand, that a low number of presence data (14) is sufficient enough to obtain a good performance of the models as long as a wide geographical area is encompassed to avoid local specificities in the training process. Moreover, in shallow environments, characterised by a diversity of environmental conditions and limited human impact, we advocate for the use of highly protected zones (such as the Gulf of Lion MPAs) as sentinel sites, to allow for the monitoring of the factors shaping the distribution of gorgonians in coastal areas. Indeed, gorgonians are known to be sensitive to mechanical impacts such as mooring (Broad

et al., 2020), bottom fishing (Bavestrello et al., 1997; Betti et al., 2020), scuba diving (Coma & Zabala, 1994) and even direct exploitation (i.e. *C. rubrum* for jewellery (Tsounis et al., 2010, 2013). The limited presence observations taken from MPA species inventories, that were repeated over time, was enough data for us to understand the habitat preferences of these species. In the present study, true absence and presence data were defined based on repeated inventories obtained between 2013 and 2021 and used to assess model accuracy. Using absence data from observations over a limited time frame should be avoided because transient population accidents may occur and absence data does not necessarily mean unsuitable habitat. Specifically, some mortality impacted populations of *E. singularis*, as per the dataset used in the present study, the species was observed in 2013 but was absent in 2019 in some locations. Given the slow population dynamics of gorgonian species, impacted populations may take a few years to recover (Linares et al., 2007). The reiteration of sampling over time is thus essential, in order to assess the ENMs performance. In addition, an observation strategy that is focused on a limited number of locations would improve the measurement of predictors by equipping sentinel sites with adequate sensors (e.g seawater temperature measurement networks such as T-MEDNet).

The limited number of observations required by ecological niche modelling algorithms (such as Maxent) allows one to extend the projections of habitat suitability to mesophotic areas and to test their capability to shelter healthy populations that can play a fundamental role in the resilience of shallow ones by providing a source of larvae (Sanchez et al., 2019; Soares et al., 2020). To achieve a good model performance, mesophotic prospections, which are limited by technological and economic constraints, would require a selection of sites sufficiently distant from each other in order to avoid spatial auto-correlation (Luoto et al., 2005; Pearson et al., 2006) and characterised by a variety of environmental conditions (Merow et al., 2013).

For all species, the suitable habitat prediction area was greater than the original inventory range. As explained above, suitable habitat is, by definition, expected to extend beyond actual presence observations and repeated observations in time are key to the fine tuning of true absence data and model accuracy. However, in the present study, while *E. cavolini* and *E. singularis* displayed very different presence distributions, their predicted suitable habitats were very similar and were identified by close predictors. Shared environmental predictors and suitable habitat between *E. cavolini* and *E. singularis* is congruent with the results of a phylogenetic study which showed evidence of hybridization or incomplete lineage sorting between the two morphologically different species (Aurelle et al., 2017). The same phylogenetic study suggested that differentiation may have resulted from isolation in different refugia during the last glaciation (Aurelle et al., 2017). In such a hypothesis, the absence of *E. cavolini* from the Gulf of Lion (except one locality in ARES) could be attributed to a quicker re-colonisation of the shallow suitable habitat by *E. singularis* after the last glaciation. Beyond the definition of a suitable habitat based on environmental or topographical predictors (potential niche), actual species distribution (realized niche) ultimately depends on efficient colonization. For sessile species, colonization can only happen during reproduction thanks to larval dispersal (Scheltema, 1971). Differences in demographic connectivity between glaciation refugia locations and the Gulf of Lion shallow habitat of the two *Eunicella* species could be an explanation for the different species current distribution. However, demographic connectivity is a complex process that operates at multiple spatial and temporal scales, resulting from species demography (population size, structure, fecundity) and larval dispersal (larval release timing, ocean currents, pelagic larval duration, larval behaviour). Differences in larval traits such as buoyancy and swimming behaviour were observed between *E. singularis*, *P. clavata* and *C. rubrum* which would explain different connectivity patterns in the same ocean currents background (Guizien et al., 2012, 2020). However, inferring connectivity patterns after the last glaciation remains speculative as larval traits have likely evolved (Wellington, 2001) and ocean currents have profoundly changed (Lynch-Stieglitz et al., 2007).

Conclusion

Accuracy and sensitivity of the suitable habitat models presented in the current study was high for four of the five species. These models can be used to complement the delineation of *P. clavata*, *C. rubrum*, *E. singularis* and *L. sarmentosa* suitable habitat in the shallow rocky bottoms along the entire Mediterranean basin and guide marine spatial planning, including the establishment of new MPAs. However, observations in the mesophotic and aphotic environments should be added to the models developed here for the shallow rocky bottoms and should be updated to incorporate more direct predictors (i.e. light, sedimentation rate, organic matter content, and sea bottom temperature) in order to avoid the use of proxies such as depth, sea surface temperature and turbidity.

Acknowledgements. This work was funded by the French National Program LITEAU IV of the Ministère de l'Ecologie et de l'Environnement Durable under project RocConnect - Connectivité des habitats rocheux fragmentés du Golfe du Lion (PI, K. Guizien, Project Number 12-MUTS-LITEAU-1-CDS-013), by the EC Interreg Marittimo program under project IMPACT - IMpatto Portuale su aree marine protette: Azioni Cooperative Transfrontaliere (PI, M. Magaldi; Ecology Task Leader, K. Guizien; CUP B12F17000370005), and by the Agence de l'Eau Rh\ône-Méditerranée-Corse under project ICONE - Impacts actuels et potentiels de la CONnectivité Ecologique ajoutée par les récifs artificiels sur la biodiversité fixée des substrats durs du Golfe du Lion (PI, K. Guizien, AAP 2016). The authors gratefully acknowledge the helpful assistance during sampling of R. Bricout, B. Hesse, L. Lescure, J.-C. Roca, and the staff of the Aire Marine Protégée Agathoise, the Réserve Nationale Marine de Cerbère-Banyuls and the Parc marin de la côte bleue. Thanks to the SHOM (https://diffusion.shom.fr/) for the LITTO3D lidar data and the OFB , the Aire Marine Protégée Agathoise, the Reserve Nationale de Cerbères-banyuls and the Parc marin de la côte bleue for the multibeam sonar data and the habitat maps. Thanks to NASA Goddard Space Flight Center, Ocean Ecology Laboratory, Ocean Biology Processing Group; (2018): Sea-viewing Wide Field-of-view Sensor (SeaWiFS) Ocean Color Data, NASA

OB.DAAC. doi: 10.5067/ORBVIEW-2/SEAWIFS/L2/OC/2018. Accessed on 06/06/2017 and 20/05/2022 for AQUAMODIS data.

Authors contributions

SB and KG conceived the study, SB and LB carried out sampling and SB did the statistical analysis. All contributed to manuscript writing.

Conflict of interest disclosure

The authors of this preprint declare that they have no financial conflict of interest with the content of this article.

LITERATURE CITED

Allouche, O., Tsoar, A., Kadmon, R., 2006. Assessing the accuracy of species distribution models: Prevalence, kappa and the true skill statistic (TSS): Assessing the accuracy of distribution models. *Journal of Applied Ecology*, *43*(6), 1223–1232. https://doi.org/10.1111/j.1365-2664.2006.01214.x

Anderson, R., DudÍk, M., Schapire, R., Blair, M., 2017. Opening the black box: An open-source release of Maxent. *Ecography*, *40*. https://doi.org/10.1111/ecog.03049

Aurelle, D., Pivotto, I. D., Malfant, M., Topcu, N. E., Masmoudi, M. B., *et al*., 2017. Fuzzy species limits in Mediterranean gorgonians (Cnidaria, Octocorallia): Inferences on speciation processes. *Hyper Article En Ligne - Sciences de l'Homme et de La Société*. https://doi.org/10.1111/zsc.12245

Bailey, M., 2010. Ecosystem-based Management for the Oceans edited by Karen McLeod and Heather Leslie (2009), xxii + 368 pp., Island Press, Washington, DC, USA. ISBN 9781597261548 (hbk), USD 90; 9781597261555 (pbk), USD 45. *Oryx*, *44*(2), 304–305. https://doi.org/10.1017/S0030605310000244

Ballesteros, E., 2006. Mediterranean coralligenous assemblages: A synthesis of present knowledge. *Oceanography and Marine Biology*, *44*, 123–195.

Bally, M., Garrabou, J., 2007. Thermodependent bacterial pathogens and mass mortalities in temperate benthic communities: A new case of emerging disease linked to climate change. *Global Change Biology*, *13*(10), 2078–2088. https://doi.org/10.1111/j.1365-2486.2007.01423.x

Bargain, A., Foglini, F., Pairaud, I., Bonaldo, D., Carniel, S., *et al.*, 2018. Predictive habitat modeling in two Mediterranean canyons including hydrodynamic variables. *Progress in Oceanography*, *169*, 151–168. https://doi.org/10.1016/j.pocean.2018.02.015

Bavestrello, G., Cerrano, C., Zanzi, D., Cattaneo-Vietti, R., 1997. Damage by fishing activities to the Gorgonian coral Paramuricea clavata in the Ligurian Sea. *Aquatic Conservation: Marine and Freshwater Ecosystems*, *7*(3), 253–262. https://doi.org/10.1002/(SICI)1099-0755(199709)7:3<253::AID-AQC243>3.0.CO;2-1

Betti, F., Bavestrello, G., Bo, M., Ravanetti, G., Enrichetti, F., *et al.*, 2020. Evidences of fishing impact on the coastal gorgonian forests inside the Portofino MPA (NW Mediterranean Sea). *Ocean & Coastal Management*, *187*, 105105. https://doi.org/10.1016/j.ocecoaman.2020.105105

Betti, F., Bo, M., Bava, S., Faimali, M., Bavestrello, G., 2018. Shallow-water sea fans: The exceptional assemblage of *Leptogorgia sarmentosa* (Anthozoa: Gorgoniidae) in the Genoa harbour (Ligurian Sea). *The European Zoological Journal*, *85*(1), 290–298. https://doi.org/10.1080/24750263.2018.1494219

Bianconi, C.H., Rivoire, G., Stiller A., Boudouresque C.F., 1988. Le corail rouge *Corallium rubrum* (Lamarck) dans la réserve naturelle de Scandola.Trav.sci. P.N.R.C., n°16 :1-83

Bo, M., Canese, S., Spaggiari, C., Pusceddu, A., Bertolino, M., *et al.*, 2012. Deep Coral Oases in the South Tyrrhenian Sea. *PLOS ONE*, *7*(11), e49870. https://doi.org/10.1371/journal.pone.0049870

Bo, M., Numa, C., del Mar Otero, M., Orejas, C., Garrabou, J., *et al.*, 2017. *Overview of the conservation status of Mediterranean anthozoa*. IUCN International Union for Conservation of Nature. https://doi.org/10.2305/IUCN.CH.2017.RA.2.en

Boavida, J., Assis, J., Silva, I., Serrão, E. A., 2016. Overlooked habitat of a vulnerable gorgonian revealed in the Mediterranean and Eastern Atlantic by ecological niche modelling. *Scientific Reports*, *6*(1), 36460. https://doi.org/10.1038/srep36460

Bongaerts, P., Ridgway, T., Sampayo, E. M., Hoegh-Guldberg, O., 2010. Assessing the 'deep reef refugia' hypothesis: Focus on Caribbean reefs. *Coral Reefs*, *29*(2), 309–327. https://doi.org/10.1007/s00338-009-0581-x

Brandl, S. J., Hoey, A. S., Bellwood, D. R., 2014. Micro-topography mediates interactions between corals, algae, and herbivorous fishes on coral reefs. *Coral Reefs*, *33*, 421–430. https://doi.org/10.1007/s00338-013-1110-5

Briton, F., Cortese, D., Duhaut, T., Guizien, K., 2018. High-resolution modelling of ocean circulation can reveal retention spots important for biodiversity conservation. *Aquatic Conservation: Marine and Freshwater Ecosystems*, *28*(4), 882–893. https://doi.org/10.1002/aqc.2901

Broad, A., Rees, M. J., Davis, A. R., 2020. Anchor and chain scour as disturbance agents in benthic environments: Trends in the literature and charting a course to more sustainable boating and shipping. *Marine Pollution Bulletin*, *161*(Pt A), 111683. https://doi.org/10.1016/j.marpolbul.2020.111683

Carleton, J. H., Sammarco, P., 1987. Effects of Substratum Irregularity on Success of Coral Settlement: Quantification by Comparative Geomorphological Techniques. *Bulletin of Marine Science*, *40*, 85–98.

Carpine, C., Grasshoff, M. , 1975. *Les Gorgonaires de la Méditerranée*. Musée océanographique.

Carrasco, P. C. (2010). Nugget effect, artificial or natural? *Journal of the Southern African Institute of Mining and Metallurgy*, *110*, 299–305.

Carugati, L., Moccia, D., Bramanti, L., Cannas, R., Follesa, M. C., *et al.*, 2022. Deep-Dwelling Populations of Mediterranean *Corallium rubrum and Eunicella cavolini*: Distribution, Demography, and Co-Occurrence. *Biology*, *11*(2), Article 2. https://doi.org/10.3390/biology11020333

Carugati, L., Moccia, D., Cau, A., Bramanti, L., Cannas, R., *et al.*, 2021. *Corallium rubrum* and *Eunicella cavolini*: Distribution, population structure and co-occurrence in the deep Mediterranean Sea. *2021 International Workshop on Metrology for the Sea; Learning to Measure Sea Health Parameters (MetroSea)*, 95–99. https://doi.org/10.1109/MetroSea52177.2021.9611596

Cau, A., Bramanti, L., Cannas, R., Follesa, M. C., Angiolillo, M., *et al.*, 2016. Habitat constraints and self-thinning shape Mediterranean red coral deep population structure: Implications for conservation practice. *Scientific Reports*, *6*(1), 23322. https://doi.org/10.1038/srep23322

Charbonnier, D., Garcia, S., 1984. Report of the technical consultation on red coral resources of the Western Mediterranean and their rational exploitation. - FA0 Fisheries Report No. 306, Rome, 1 - 142.

Cocito, S., Bedulli, D., Sgorbini, S., 2002. Distribution patterns of the sublittoral epibenthic assemblages on a rocky shoal in the Ligurian Sea (NW Mediterranean). *Scientia Marina*, *66*(2), 175–181. https://doi.org/10.3989/scimar.2002.66n2175

Coma, R., Linares, C., Ribes, M., Diaz, D., Garrabou, J., *et al.*, 2006. Consequences of a mass mortality in populations of *Eunicella singularis* (Cnidaria: Octocorallia) in Menorca (NW Mediterranean). *Marine Ecology Progress Series*, *327*, 51–60. https://doi.org/10.3354/meps327051

Coma, R., Ribes, M., Zabala, M., Giti, J.-M., 1995. Reproduction and cycle of gonadal development in the Mediterranean gorgonian *Paramuricea clavata*. *Marine Ecology Progress Series*, *117*, 173–183. https://doi.org/10.3354/meps117173

Coma, R., Zabala, M., 1994. Efecto de la frequentacion sobre las poblaciones de *Paramuricea clavata* en las illes Medes. In : Resumenes del VIII Simposio Iberico de Estudios del Bentos Marino, Blanes, Spain, 170-171.

Costantini, F., Gori, A., Lopez-González, P., Bramanti, L., Rossi, S., *et al*., 2016. Limited genetic connectivity between gorgonian morphotypes along a depth gradient. *11*(8). https://doi.org/10.1371/journal.pone.0160678

Di Camillo, C. G., Ponti, M., Bavestrello, G., Krzelj, M., Cerrano, C., 2018. Building a baseline for habitat-forming corals by a multi-source approach, including Web Ecological Knowledge. *Biodiversity and Conservation*, *27*(5), 1257–1276. https://doi.org/10.1007/s10531-017-1492-8

Dolan, M. F. J., Grehan, A. J., Guinan, J. C., Brown, C., 2008. Modelling the local distribution of cold-water corals in relation to bathymetric variables: Adding spatial context to deep-sea video data. *Deep Sea Research Part I: Oceanographic Research Papers*, *55*(11), 1564–1579. https://doi.org/10.1016/j.dsr.2008.06.010

Elith, J., H. Graham, C., P. Anderson, R., Dudík, M., Ferrier, S., *et al*., 2006. Novel methods improve prediction of species' distributions from occurrence data. *Ecography*, *29*(2), 129–151. https://doi.org/10.1111/j.2006.0906-7590.04596.x

Elith, J., Phillips, S. J., Hastie, T., Dudík, M., *et al*., 2011. A statistical explanation of MaxEnt for ecologists. *Diversity and Distributions*, *17*(1), 43–57. https://doi.org/10.1111/j.1472-4642.2010.00725.x

EVANS, I. S., 1980. An integrated system of terrain analysis and slope mapping. *An Integrated System of Terrain Analysis and Slope Mapping*, *36*, 274–295.

Ezzat, L., Merle, P.-L., Furla, P., Buttler, A., Ferrier-Pagès, C., 2013. The Response of the Mediterranean Gorgonian *Eunicella singularis* to Thermal Stress Is Independent of Its Nutritional Regime. *PLOS ONE*, *8*(5), e64370. https://doi.org/10.1371/journal.pone.0064370

Forcioli, D., Merle, P.-L., Caligara, C., Ciosi, M., Muti, C., *et al.*, 2011. Symbiont diversity is not involved in depth acclimation in the Mediterranean sea whip *Eunicella singularis*. *Marine Ecology Progress Series*, *439*, 57–71. https://doi.org/10.3354/meps09314

Fourt, M., Goujard, A., Pérez, T., Chevaldonné, P., 2017. Guide de la faune profonde de la mer Méditerranée : Explorations des roches et canyons sous-marins des côtes françaises. Muséum national d'Histoire naturelle, Paris, 184p. (Patrimoines naturels ; 75).

Garrabou, J., Coma, R., Bensoussan, N., Bally, M., Chevaldonné, P., *et al.*, 2009. Mass mortality in Northwestern Mediterranean rocky benthic communities: Effects of the 2003 heat wave. *Global Change Biology*, *15*(5), 1090–1103. https://doi.org/10.1111/j.1365-2486.2008.01823.x

Garrabou, J., Perez, T., Sartoretto, S., Harmelin, J., 2001. Mass mortality event in red coral *Corallium rubrum* populations in the Provence region (France, NW Mediterranean). *Marine Ecology Progress Series*, *217*, 263–272. https://doi.org/10.3354/meps217263

Georgiadis, M., Papatheodorou, G., Tzanatos, E., Geraga, M., Ramfos, A., *et al.*, 2009. Coralligène formations in the eastern Mediterranean Sea: Morphology, distribution, mapping and relation to fisheries in the southern Aegean Sea (Greece) based on high-resolution acoustics. *Journal of Experimental Marine Biology and Ecology*, *368*(1), 44–58. https://doi.org/10.1016/j.jembe.2008.10.001

Gili, J.-M., Coma, R., 1998. Benthic suspension feeders: Their paramount role in littoral marine food webs. *Trends in Ecology & Evolution*, *13*, 316–321. https://doi.org/10.1016/S0169-5347(98)01365-2

Glasby, T. M., 2000. Surface composition and orientation interact to affect subtidal epibiota. *Journal of Experimental Marine Biology and Ecology*, *248*(2), 177–190. https://doi.org/10.1016/S0022-0981(00)00169-6

Gohin, F., Bryère, P., Lefebvre, A., Sauriau, P.-G., Savoye, N., *et al.*, 2020. Satellite and In Situ Monitoring of Chl-a, Turbidity, and Total Suspended Matter in Coastal Waters: Experience of

the Year 2017 along the French Coasts. *Journal of Marine Science and Engineering*, *8*(9), 665. https://doi.org/10.3390/jmse8090665

Gori, A., Bramanti, L., López-González, P., Thoma, J. N., Gili, J.-M., *et al.*, 2012. Characterization of the zooxanthellate and azooxanthellate morphotypes of the Mediterranean gorgonian *Eunicella singularis*. *Marine Biology*, *159*(7), 1485–1496. https://doi.org/10.1007/s00227-012-1928-3

Gori, A., Rossi, S., Berganzo, E., Pretus, J. L., Dale, M. R. T., *et al.*, 2011. Spatial distribution patterns of the gorgonians *Eunicella singularis*, *Paramuricea clavata*, and *Leptogorgia sarmentosa* (Cape of Creus, Northwestern Mediterranean Sea). *Marine Biology*, *158*(1), 143–158. https://doi.org/10.1007/s00227-010-1548-8

Grinyó, J., Gori, A., Ambroso, S., Purroy, A., Calatayud, C., *et al.*, 2016. Diversity, distribution and population size structure of deep Mediterranean gorgonian assemblages (Menorca Channel, Western Mediterranean Sea). *Progress in Oceanography*, *145*, 42–56. https://doi.org/10.1016/j.pocean.2016.05.001

Guinan, J., Brown, C., Dolan, M. F. J., Grehan, A. J., 2009. Ecological niche modelling of the distribution of cold-water coral habitat using underwater remote sensing data. *Ecological Informatics*, *4*(2), 83–92. https://doi.org/10.1016/j.ecoinf.2009.01.004

Guizien, K., Belharet, M., Marsaleix, P., Guarini, J. M., 2012. Using larval dispersal simulations for marine protected area design: Application to the Gulf of Lions (northwest Mediterranean). *Limnology and Oceanography*, *57*(4), 1099–1112. https://doi.org/10.4319/lo.2012.57.4.1099

Guizien, K., Bramanti, L., Roca, J.-C., Hesse, B., Blouet, S., *et al.*, 2022. *Database of sea fans spatial distribution in the northwestern Mediterranean sea* [Data set]. SEANOE. https://doi.org/10.17882/86176

Guizien, K., Viladrich, N., Martínez-Quintana, Á., Bramanti, L., 2020. Survive or swim: Different relationships between migration potential and larval size in three sympatric Mediterranean octocorals. *Scientific Reports*, *10*(1), Article 1. https://doi.org/10.1038/s41598-020-75099-1

Hamon, M., Beuvier, J., Somot, S., Lellouche, J.-M., *et al.*, 2016. Design and validation of MEDRYS, a Mediterranean Sea reanalysis over the period 1992–2013. *Ocean Science*, *12*(2), 577–599. https://doi.org/10.5194/os-12-577-2016

Hanley, J. A., McNeil, B. J., 1982. The meaning and use of the area under a receiver operating characteristic (ROC) curve. *Radiology*, *143*(1), 29–36. https://doi.org/10.1148/radiology.143.1.7063747

Hernandez, P. A., Franke, I., Herzog, S. K., Pacheco, V., Paniagua, L., *et al.*, 2008. Predicting species distributions in poorly-studied landscapes. *Biodiversity and Conservation*, *17*(6), 1353–1366. https://doi.org/10.1007/s10531-007-9314-z

Hernandez, P. A., Graham, C. H., Master, L. L., Albert, D. L., 2006. The effect of sample size and species characteristics on performance of different species distribution modeling methods. *Ecography*, *29*(5), 773–785. https://doi.org/10.1111/j.0906-7590.2006.04700.x

Hiscock, K., 1983. Water movement. Chapter 3, p. 58-96 in Earll & Erwin 1983

Horta e Costa, B., Claudet, J., Franco, G., Erzini, K., Caro, A., *et al.*, 2016. A regulation-based classification system for Marine Protected Areas (MPAs). *Marine Policy*, *72*, 192–198. https://doi.org/10.1016/j.marpol.2016.06.021

Jarnevich, C. S., Holcombe, T. R., Thomas, C. C., Frid, L., Olsson, A., 2015. Simulating long-term effectiveness and efficiency of management scenarios for an invasive grass. *AIMS Environmental Science*, *2*(2), 427–447. https://doi.org/10.3934/environsci.2015.2.427

Knott, N. A., Underwood, A. J., Chapman, M. G., Glasby, T. M., 2004. Epibiota on vertical and on horizontal surfaces on natural reefs and on artificial structures. *Journal of the Marine Biological Association of the United Kingdom*, *84*(6), 1117–1130. https://doi.org/10.1017/S0025315404010550h

Laborel, J., 1960. Contribution à l'étude directe des peuplements benthiques sciaphiles sur substrats rocheux en Méditerranée. Rec. Trav. St. mar. Endoume 33 (20):117-173

La Rivière, M., Michez, N., Delavenne, J., Andres, S., Fréjefond, C., *et al.*, 2021. Fiches descriptives des biocénoses benthiques de Méditerranée. UMS PatriNat (OFB-CNRS-MNHN), Paris : 660 pp.

Legendre, P., Dale, M. R. T., Fortin, M.-J., Gurevitch, J., Hohn, M., *et al.*, 2002. The consequences of spatial structure for the design and analysis of ecological field surveys. *Ecography*, *25*(5), 601–615. https://doi.org/10.1034/j.1600-0587.2002.250508.x

Leversee, G. J., 1976. Flow and feeding in fan-shaped colonies of the gorgonian coral, *Leptogorgia*. *The Biological Bulletin*, *151*(2), 344–356. https://doi.org/10.2307/1540667

Liew, S. C., Saengtuksin, B., Kwoh, L. K., 2009. Monitoring turbidity and suspended sediment concentration of coastal and inland waters using satellite data. *2009 IEEE International Geoscience and Remote Sensing Symposium*, *2*, II-837-II–839. https://doi.org/10.1109/IGARSS.2009.5418225

Linares, C., Coma, R., Garrabou, J., Díaz, D., Zabala, M., 2008. Size distribution, density and disturbance in two Mediterranean gorgonians: *Paramuricea clavata* and *Eunicella singularis*. *Journal of Applied Ecology*, *45*(2), 688–699. https://doi.org/10.1111/j.1365-2664.2007.01419.x

Linares, C., Doak, D. F., Coma, R., Díaz, D., Zabala, M., 2007. Life history and viability of a long-lived marine invertebrate: the octocoral *Paramuricea clavata*. *Ecology*, *88*(4), 918–928. https://doi.org/10.1890/05-1931

Liu, C., Berry, P. M., Dawson, T. P., Pearson, R. G., 2005. Selecting thresholds of occurrence in the prediction of species distributions. *Ecography*, *28*(3), 385–393. https://doi.org/10.1111/j.0906-7590.2005.03957.x

Lo Iacono, C., Robert, K., Gonzalez-Villanueva, R., Gori, A., Gili, J.-M., *et al.*, 2018. Predicting cold-water coral distribution in the Cap de Creus Canyon (NW Mediterranean): Implications for marine conservation planning. *Progress in Oceanography*, *169*, 169–180. https://doi.org/10.1016/j.pocean.2018.02.012

Lorenzo, B., Ilaria, V., Sergio, R., Stefano, S., Giovanni, S., 2011. Involvement of recreational scuba divers in emblematic species monitoring: The case of Mediterranean red coral (*Corallium rubrum*). *Journal for Nature Conservation*, *19*(5), 312–318. https://doi.org/10.1016/j.jnc.2011.05.004

Luoto, M., Pöyry, J., Heikkinen, R. K., Saarinen, K., 2005. Uncertainty of bioclimate envelope models based on the geographical distribution of species. *Global Ecology and Biogeography*, *14*, 575–584. https://doi.org/10.1111/j.1466-822x.2005.00186.x

Lynch-Stieglitz, J., Adkins, J. F., Curry, W. B., Dokken, T., Hall, I. R., *et al.*, 2007. Atlantic Meridional Overturning Circulation During the Last Glacial Maximum. *Science*, *316*(5821), 66–69. https://doi.org/10.1126/science.1137127

Merckx, B., Steyaert, M., Vanreusel, A., Vincx, M., Vanaverbeke, J., 2011. Null models reveal preferential sampling, spatial autocorrelation and overfitting in habitat suitability modelling. *Ecological Modelling*, *222*(3), 588–597.

Merow, C., Smith, M. J., Silander Jr, J. A., 2013. A practical guide to MaxEnt for modeling species' distributions: What it does, and why inputs and settings matter. *Ecography*, *36*(10), 1058–1069. https://doi.org/10.1111/j.1600-0587.2013.07872.x

Mistri, M., 1995. Population Structure and Secondary Production of the Mediterranean Octocoral *Lophogorgia ceratophyta* (L. 1758). *Marine Ecology*, *16*(3), 181–188. https://doi.org/10.1111/j.1439-0485.1995.tb00404.x

Mistri, M., Ceccherelli, V. U., 1993. Growth of the Mediterranean Gorgonian *Lophogorgia ceratophyta* (L., 1758). *Marine Ecology*, *14*(4), 329–340. https://doi.org/10.1111/j.1439-0485.1993.tb00004.x

Nozawa, Y., 2008. Micro-crevice structure enhances coral spat survivorship. *Journal of Experimental Marine Biology and Ecology*, *367*(2), 127–130. https://doi.org/10.1016/j.jembe.2008.09.004

Odum, E.P., 1971. An understanding of ecological succession provides a basis for resolving man's conflict with nature. *164*, 9.

Pearson, R. G., 2007. Species' Distribution Modeling for Conservation Educators and Practitioners. Synthesis America Museum of Natural History. Avaible at http://ncep.anmnh.org.

Pearson, R. G., Raxworthy, C. J., Nakamura, M., Townsend Peterson, A., 2006. ORIGINAL ARTICLE: Predicting species distributions from small numbers of occurrence records: a test case using cryptic geckos in Madagascar: Predicting species distributions with low sample sizes. *Journal of Biogeography*, *34*(1), 102–117. https://doi.org/10.1111/j.1365-2699.2006.01594.x

Perez, J.M., 1961. Océanographie biologique et biologie marine. Tome premier: la vie benthique. Paris, P.U.F. éd. : 1-541, 35 fig.

Phillips, S. J., Anderson, R. P., Schapire, R. E., 2006. Maximum entropy modeling of species geographic distributions. *Ecological Modelling*, *190*(3–4), 231–259. https://doi.org/10.1016/j.ecolmodel.2005.03.026

Phillips, S. J., Dudık, M., 2008. *Modeling of species distributions with Maxent: New extensions and a comprehensive evaluation*. Ecography 31, 161-175.

Piazzi, L., Atzori, F., Cadoni, N., Cinti, M. F., Frau, F., *et al.*, 2018. Benthic mucilage blooms threaten coralligenous reefs. *Marine Environmental Research*, *140*, 145–151. https://doi.org/10.1016/j.marenvres.2018.06.011

Ponti, M., Turicchia, E., Costantini, F., Gori, A., Bramanti, L., *et al.*, 2019. *Mediterranean gorgonian forests: Distribution patterns and ecological roles*.

Radosavljevic, A., Anderson, R., 2013. Making better MAXENT models of species distributions: Complexity, overfitting and evaluation. *Journal of Biogeography*, *41*. https://doi.org/10.1111/jbi.12227

Rossi, L., 1959. Le specie di *Eunicella* (Gorgonaria) deI golfe diGenova. Annali dei Museo civica di sioria na/urate di Genova, 71, pp. 203-225, 8 fig., pl. 8-12.

Rossi, S., Bramanti, L., Gori, A., Orejas, C. (Eds.), 2017. *Marine Animal Forests: The Ecology of Benthic Biodiversity Hotspots*. Springer International Publishing. https://www.springer.com/gp/book/9783319210117

Rossi, S., Gili, J.-M., Garrofé, X., 2011. Net negative growth detected in a population of *Leptogorgia sarmentosa*: Quantifying the biomass loss in a benthic soft bottom-gravel gorgonian. *Marine Biology*, *158*(7), 1631–1643. https://doi.org/10.1007/s00227-011-1675-x

Rossi, S., Rizzo, L., 2021. The Importance of Food Pulses in Benthic-Pelagic Coupling Processes of Passive Suspension Feeders. *Water*, *13*(7), 997. https://doi.org/10.3390/w13070997

Rossi, S., Tsounis, G., Orejas, C., Padrón, T., Gili, J. M., Bramanti, L., *et al*., 2008. Survey of deep-dwelling red coral (*Corallium rubrum*) populations at Cap de Creus (NW Mediterranean). *Marine Biology*, *154*(3), 533–545. https://doi.org/10.1007/s00227-008-0947-6

Sanchez, J., Dueñas, L., Rowley, S., Vergara, D., Montaño Salazar, S., *et al*., 2019. *Gorgonian Corals* (pp. 729–747). https://doi.org/10.1007/978-3-319-92735-0_39

Scheltema, R. S., 1971. Larval dispersal as a means of genetic exchange between geographically separated populations of shallow-water benthic marine gastropods. *The Biological Bulletin*, *140*(2), 284–322. https://doi.org/10.2307/1540075

Sempere-Valverde, J., Ostalé-Valriberas, E., Farfán, G. M., Espinosa, F., 2018. Substratum type affects recruitment and development of marine assemblages over artificial substrata: A case study in the Alboran Sea. *Estuarine, Coastal and Shelf Science*, *204*, 56–65. https://doi.org/10.1016/j.ecss.2018.02.017

Sillero, N., Arenas-Castro, S., Enriquez-Urzelai, U., Vale, C. G., Sousa-Guedes, D., *et al*., 2021. Want to model a species niche? A step-by-step guideline on correlative ecological niche modelling. *Ecological Modelling*, *456*, 109671. https://doi.org/10.1016/j.ecolmodel.2021.109671

Sini, M., Kipson, S., Linares, C., Koutsoubas, D., Garrabou, J., 2015. The Yellow Gorgonian *Eunicella cavolini*: Demography and Disturbance Levels across the Mediterranean Sea. *PLOS ONE*, 19.

Soares, M. de O., Araújo, J. T. de, Ferreira, S. M. C., Santos, B. A., Boavida, J. R. H., *et al*., 2020. Why do mesophotic coral ecosystems have to be protected? *Science of The Total Environment*, *726*, 138456. https://doi.org/10.1016/j.scitotenv.2020.138456

True, M.A., 1970. Étude quantitative de quatre peuplements sciaphiles sur substrat rocheux dans la région marsellaise. Bull. Inst. Océanogr. Monaco, 69(1401): 1-48.

Tsounis, G., Rossi, S., Bramanti, L., Santangelo, G., 2013. Management hurdles in sustainable harvesting of *Corallium rubrum*. *Marine Policy*, *39*. https://doi.org/10.1016/j.marpol.2012.12.010i

Tsounis, G., Rossi, S., Grigg, R., Santangelo, G., Bramanti, L., *et al*., 2010. The exploitation and conservation of precious corals. *Oceanogr Mar Biol Annu Rev*, *48*, 161–212.

Turicchia, E., Abbiati, M., Sweet, M., Ponti, M., 2018. Mass mortality hits gorgonian forests at Montecristo Island. *Diseases of Aquatic Organisms*, *131*(1), 79–85. https://doi.org/10.3354/dao03284

Virgilio, M., Airoldi, L., Abbiati, M., 2006. Spatial and temporal variations of assemblages in a Mediterranean coralligenous reef and relationships with surface orientation. *Coral Reefs*, *25*(2), 265–272. https://doi.org/10.1007/s00338-006-0100-2

Weinberg, S., 1978. The minimal area problem in invertebrate communities of Mediterranean rocky substrata. *Marine Biology*, *49*(1), 33–40. https://doi.org/10.1007/BF00390728

Weinberg, S., 1979a. Autecology of Shallow-Water Octocorallia from Mediterranean Rocky Substrata, I. The Banyuls Area. *Bijdragen Tot de Dierkunde*, *49*(1), 1–15. https://doi.org/10.1163/26660644-04901001

Weinberg, S., 1979b. The Light-Dependent Behaviour of Planula Larvae of *Eunicella Singularis and Corallium Rubrum* and its Implication for Octocorallian Ecology. *Bijdragen Tot de Dierkunde*, *49*(1), 16–30. https://doi.org/10.1163/26660644-04901002

Weinberg, S., Weinberg, F., 1979. The Life Cycle of a Gorgonian: *Eunicella Singularis* (Esper, 1794). *Contributions to Zoology Bijdragen Tot de Dierkunde*, *48*, 127–140. https://doi.org/10.1163/26660644-04802003

Wellington, G. M., 2001. Variation in larval life-history traits among reef ® shes across the Isthmus of Panama. 12.

White, M., Mohn, C., de Stigter, H., Mottram, G., 2005. Deep-water coral development as a function of hydrodynamics and surface productivity around the submarine banks of the Rockall Trough, NE Atlantic. In A. Freiwald & J. M. Roberts (Eds.), *Cold-Water Corals and Ecosystems* (pp. 503–514). Springer Berlin Heidelberg. https://doi.org/10.1007/3-540-27673-4_25

Wilson, M. F. J., O'Connell, B., Brown, C., Guinan, J. C., Grehan, A. J., 2007. Multiscale Terrain Analysis of Multibeam Bathymetry Data for Habitat Mapping on the Continental Slope. *Marine Geodesy*, *30*(1–2), 3–35. https://doi.org/10.1080/01490410701295962

Zweig, M.H., Campbell, G., 1993. Receiver-operating characteristic (ROC) plots: a fundamental evaluation tool in clinical medicine. Clin. Chem. 39, 561–577.

Appendices

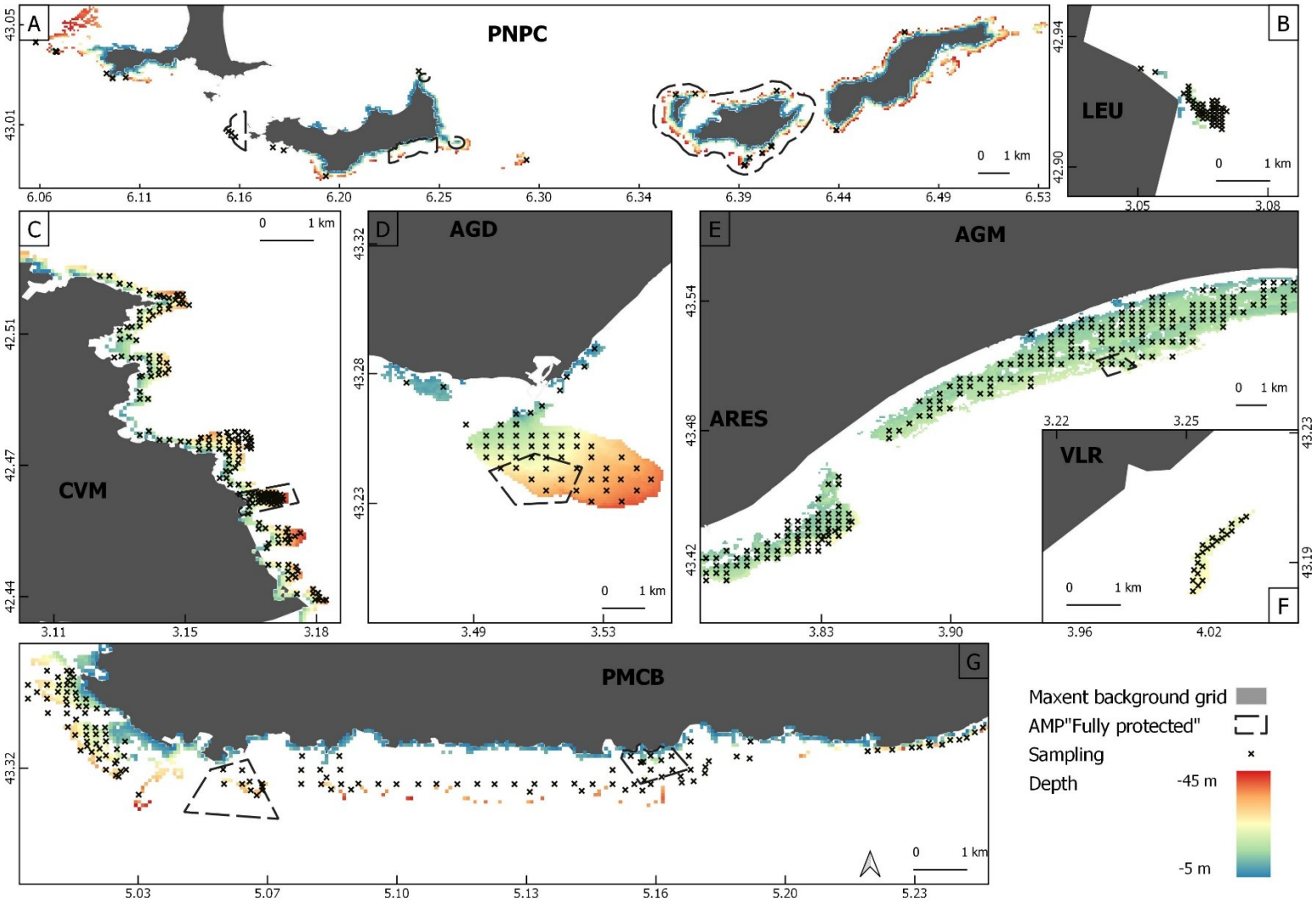
A
PNPC
B
LEU
C
CVM
D
AGD
E
AGM
ARES
F
VLR
G
PMCB
0 1 km
Maxent background grid
AMP"Fully protected"
Sampling
Depth
-45 m
-5 m

Figure S1: Sampling location and bathymetry in each of the eight sites. **A** close up PNPC, **B** close up LEU, **C** close up CVM, **D** close up AGD, **E** close up AGM and ARES, **F** closeup VLR, **G** close up PMCB.

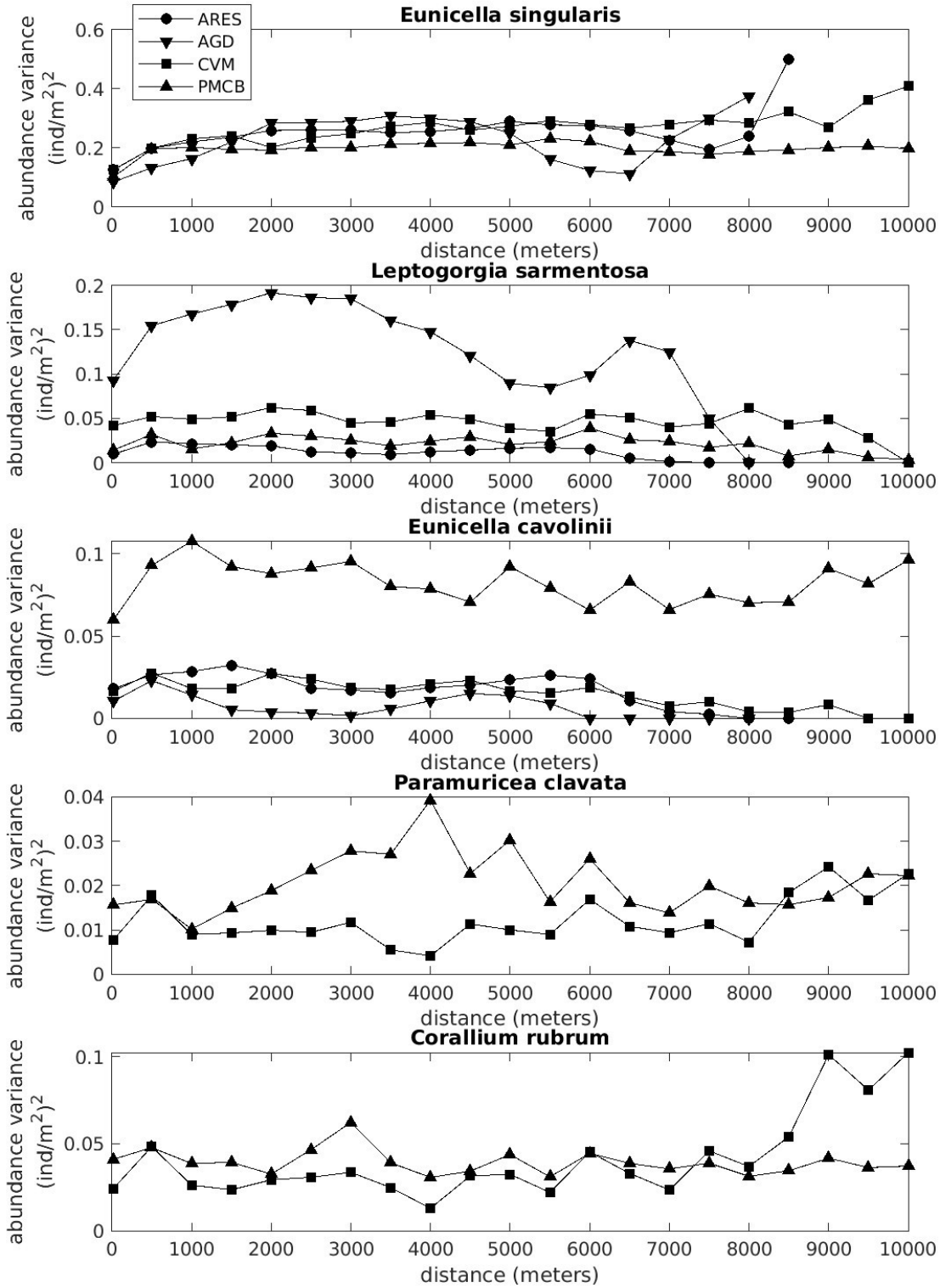
Eunicella singularis
ARES
AGD
CVM
PMCB
abundance variance (ind/m²)²
distance (meters)
Leptogorgia sarmentosa
abundance variance (ind/m²)²
distance (meters)
Eunicella cavolinii
abundance variance (ind/m²)²
distance (meters)
Paramuricea clavata
abundance variance (ind/m²)²
distance (meters)
Corallium rubrum
abundance variance (ind/m²)²
distance (meters)

Figure S2: Empirical semivariograms describing the spatial variability of each of the five gorgonian species in the four sites (ARES, AGD, CVM, PMCB) where the species was present. Semivariograms were computed using population spatial density measured in the 696 evenly spaced geo-referenced locations covering the hard bottom habitat and clustering them by distance classes ranging from 500 meters to 10 kms, with a step of 500 meters increment. The nugget of the semivariogram was computed using replicated measurements made at less than 20 meters distance, around each geo-referenced location (Guizien et al., 2022).

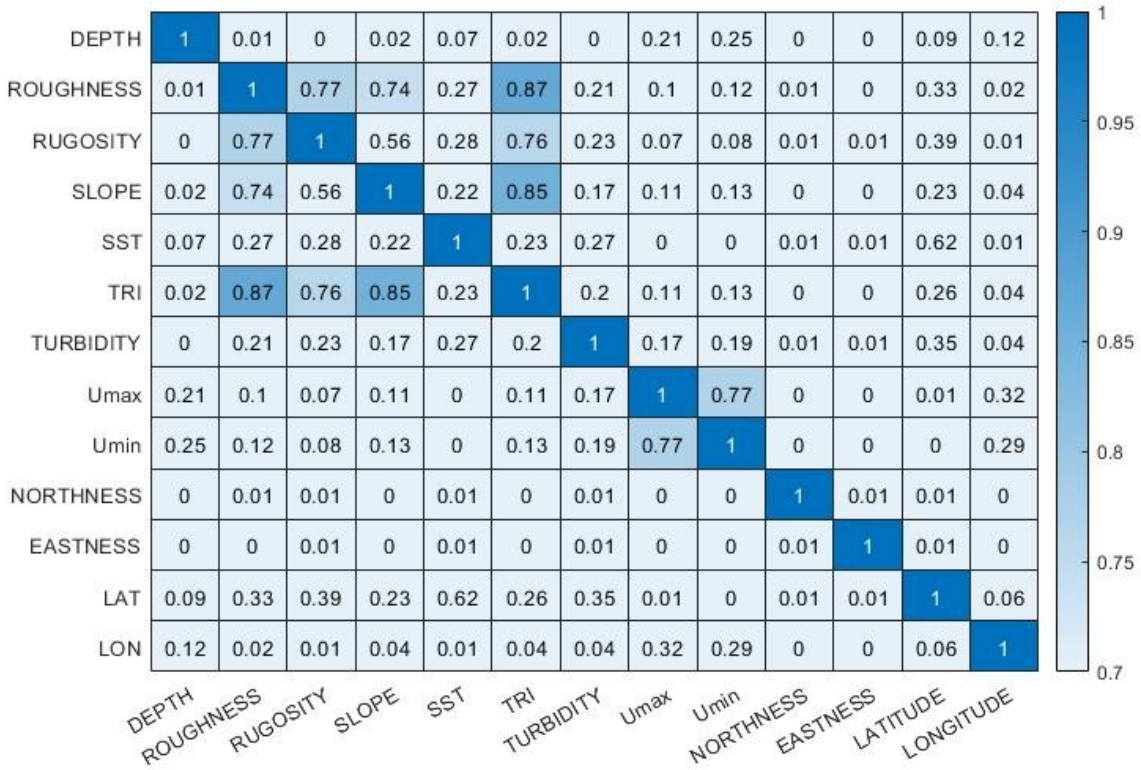

Figure S3 : Matrix of correlation (Rho spearman) on the 13 initials variables (geomorphologic, environmental, and latitude / longitude)

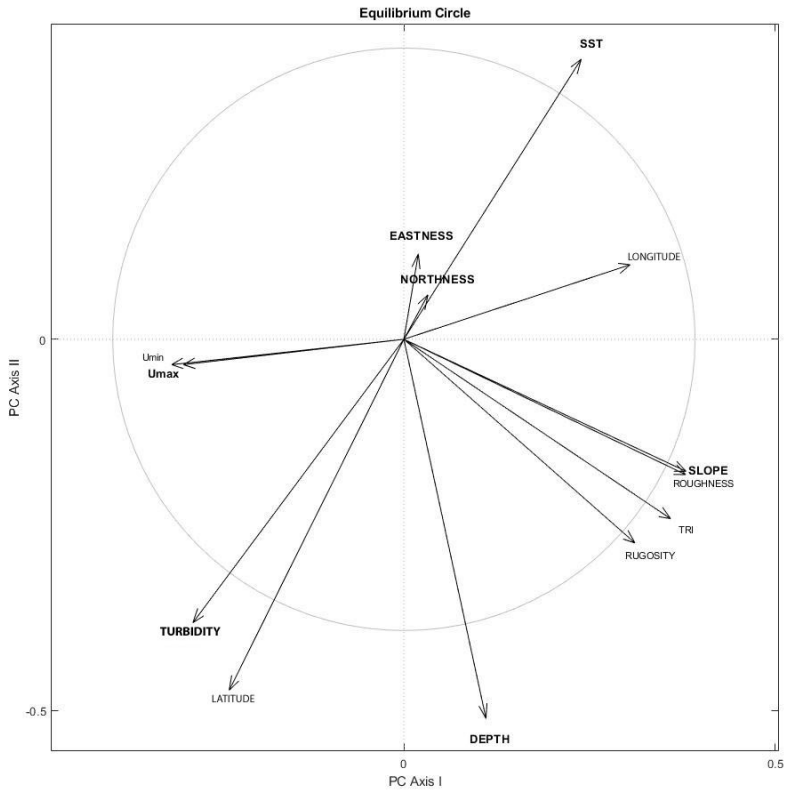

Figure S4 : Analyse of principale composante on the 13 initials variables geomorphologic, environmental, and latitude / longitude).

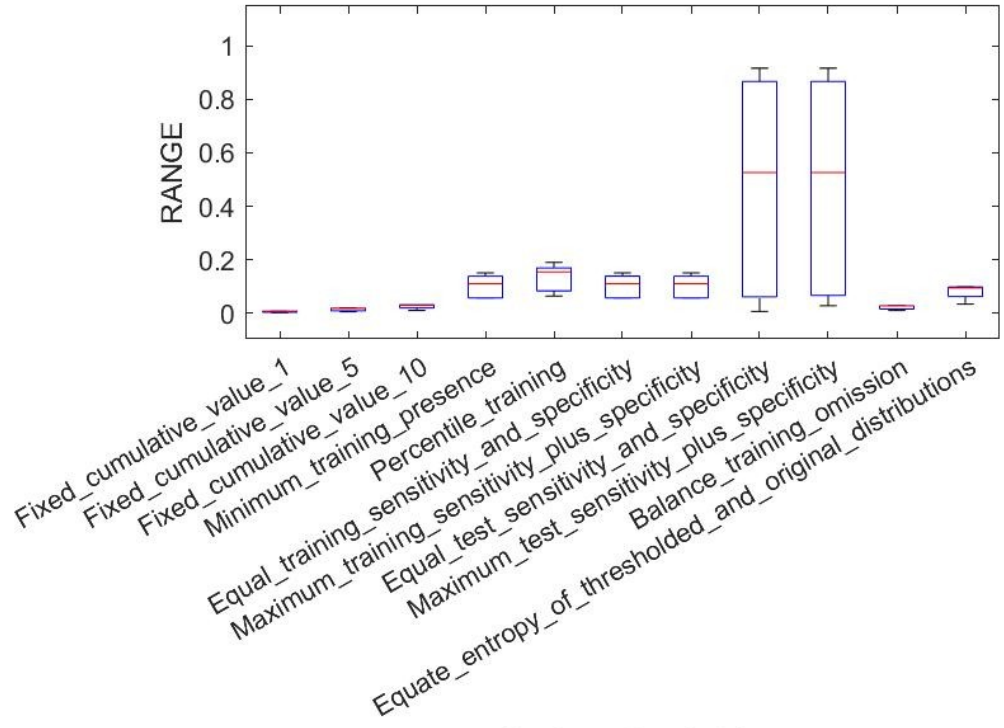

A

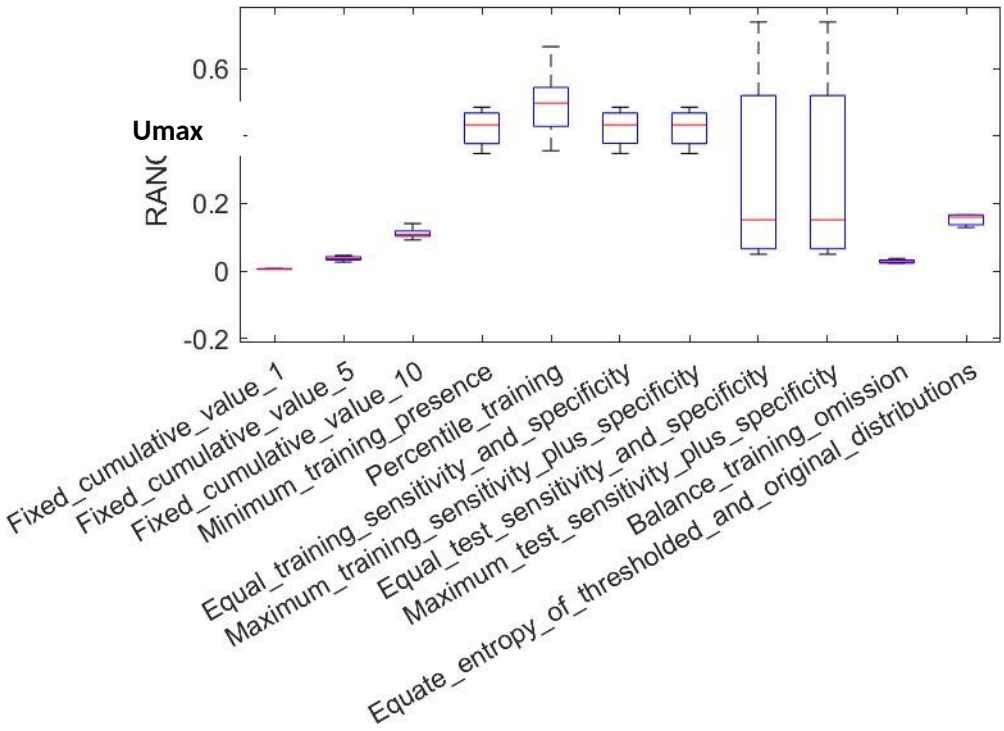

B

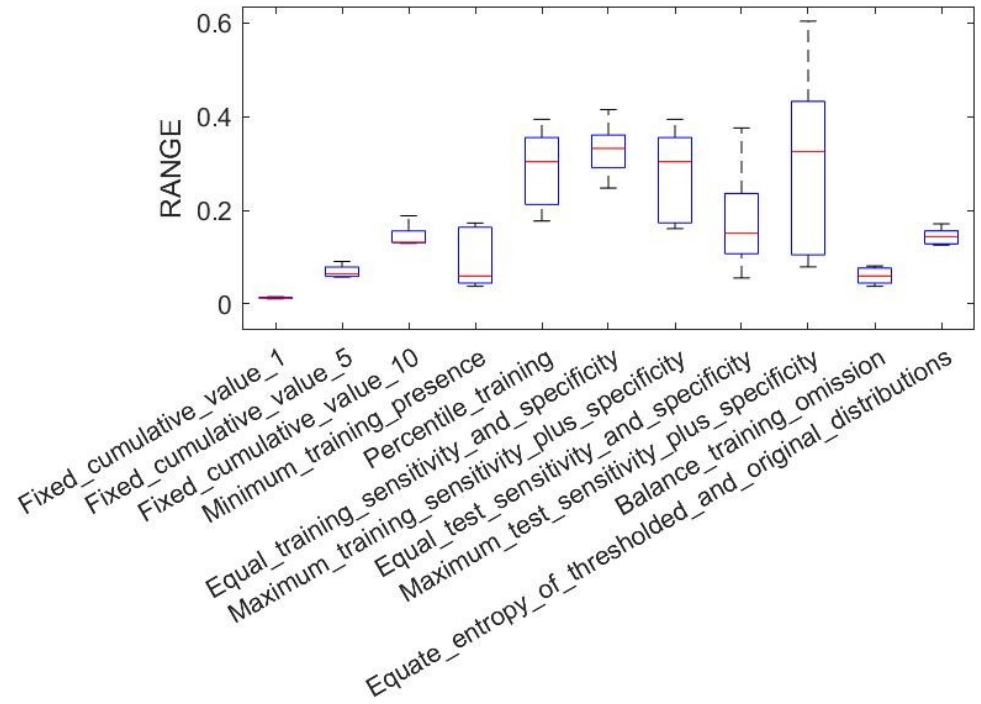
RANGE
0.6
0.4
0.2
0
Fixed_cumulative_value_1
Fixed_cumulative_value_5
Fixed_cumulative_value_10
Minimum_training_presence
Percentile_training
Equal_training_sensitivity_and_specificity
Maximum_training_sensitivity_plus_specificity
Equal_test_sensitivity_and_specificity
Maximum_test_sensitivity_plus_specificity
Balance_training_omission
Equate_entropy_of_thresholded_and_original_distributions

C

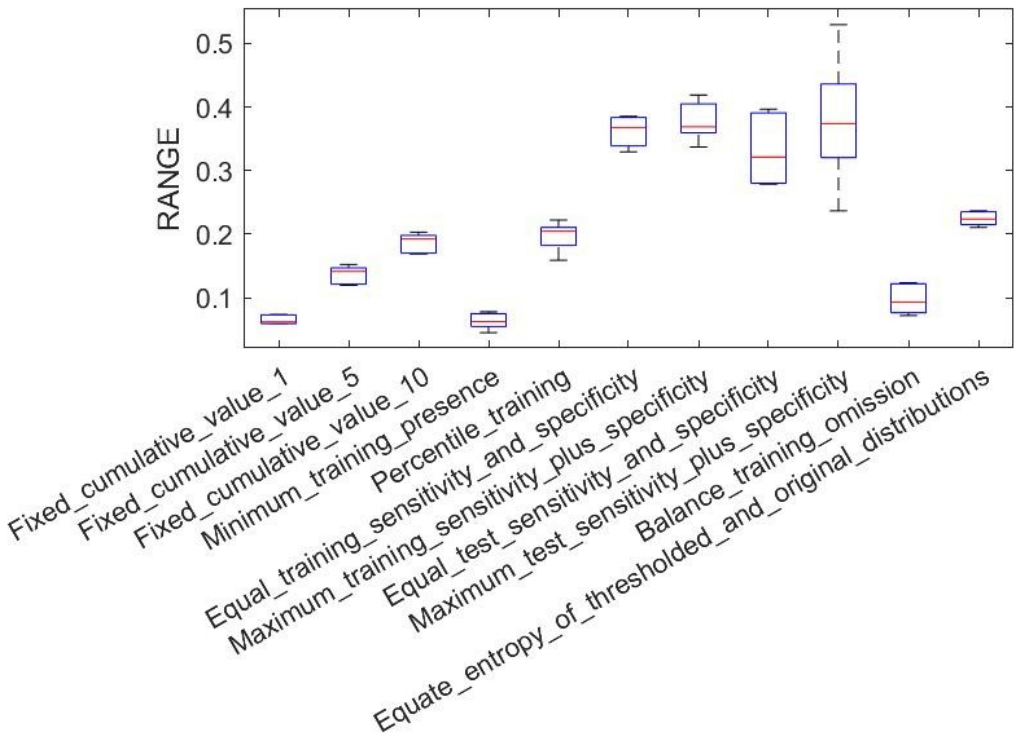
RANGE
0.5
0.4
0.3
0.2
0.1
Fixed_cumulative_value_1
Fixed_cumulative_value_5
Fixed_cumulative_value_10
Minimum_training_presence
Percentile_training
Equal_training_sensitivity_and_specificity
Maximum_training_sensitivity_plus_specificity
Equal_test_sensitivity_and_specificity
Maximum_test_sensitivity_plus_specificity
Balance_training_omission
Equate_entropy_of_thresholded_and_original_distributions

D

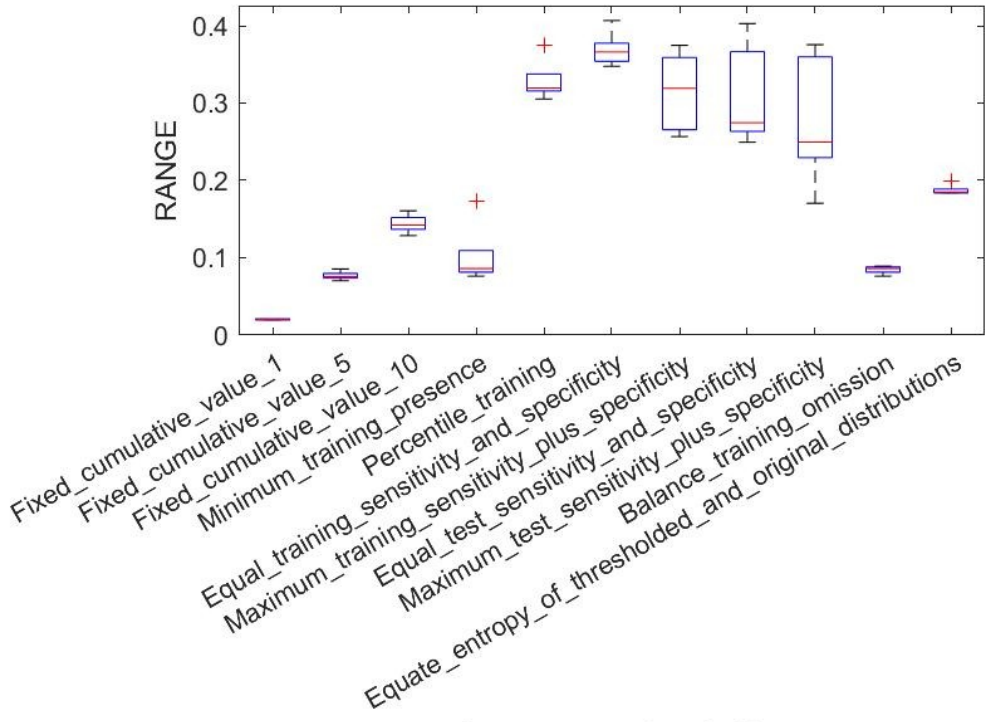

E

Figure S5: Threshold by index for the 5 species (MAXENT model). Modeling with all predictors without geographical predictors (Latitude / Longitude). **A**: *C. rubrum*, **B**: *P.clavata*, **C**: *E. cavolini*, **D**: *E.singularis*, **E**: *L. sarmentosa*

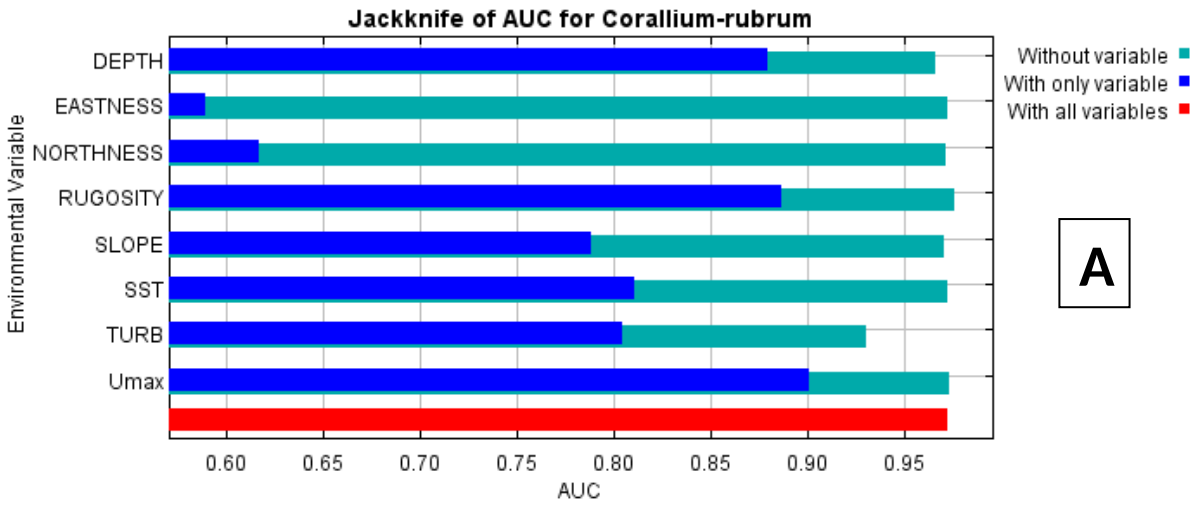
Jackknife of AUC for Corallium-rubrum
DEPTH
EASTNESS
NORTHNESS
RUGOSITY
SLOPE
SST
TURB
Umax
Environmental Variable
0.60
0.65
0.70
0.75
0.80
0.85
0.90
0.95
AUC
Without variable
With only variable
With all variables

A

B

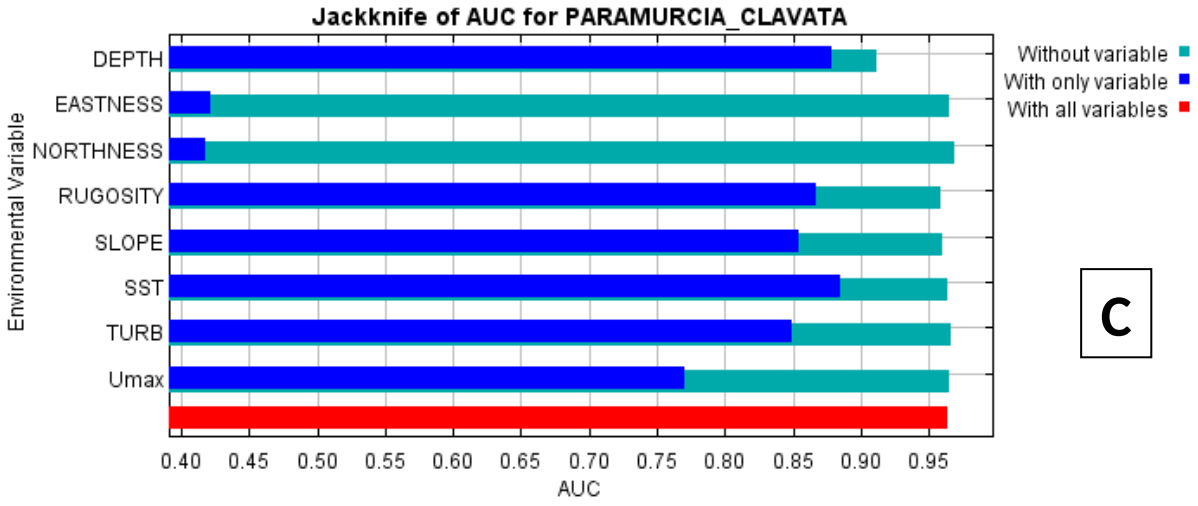
Jackknife of AUC for PARAMURCIA_CLAVATA
DEPTH
EASTNESS
NORTHNESS
RUGOSITY
SLOPE
SST
TURB
Umax
Environmental Variable
0.40
0.45
0.50
0.55
0.60
0.65
0.70
0.75
0.80
0.85
0.90
0.95
AUC
Without variable
With only variable
With all variables

C

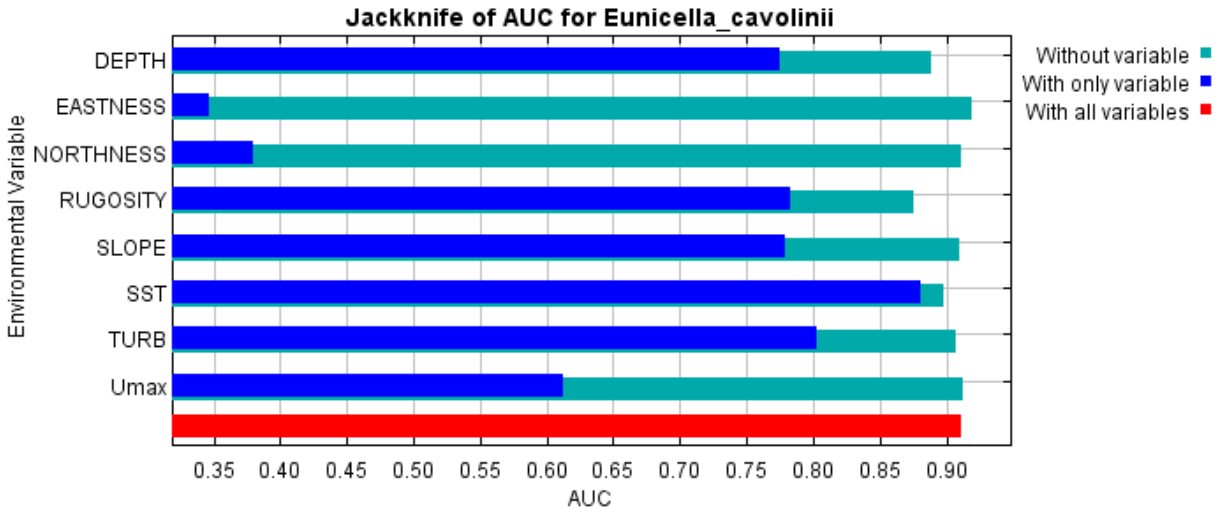
Jackknife of AUC for Eunicella_cavolinii
Environmental Variable
DEPTH
EASTNESS
NORTHNESS
RUGOSITY
SLOPE
SST
TURB
Umax
0.35
0.40
0.45
0.50
0.55
0.60
0.65
0.70
0.75
0.80
0.85
0.90
AUC
Without variable
With only variable
With all variables

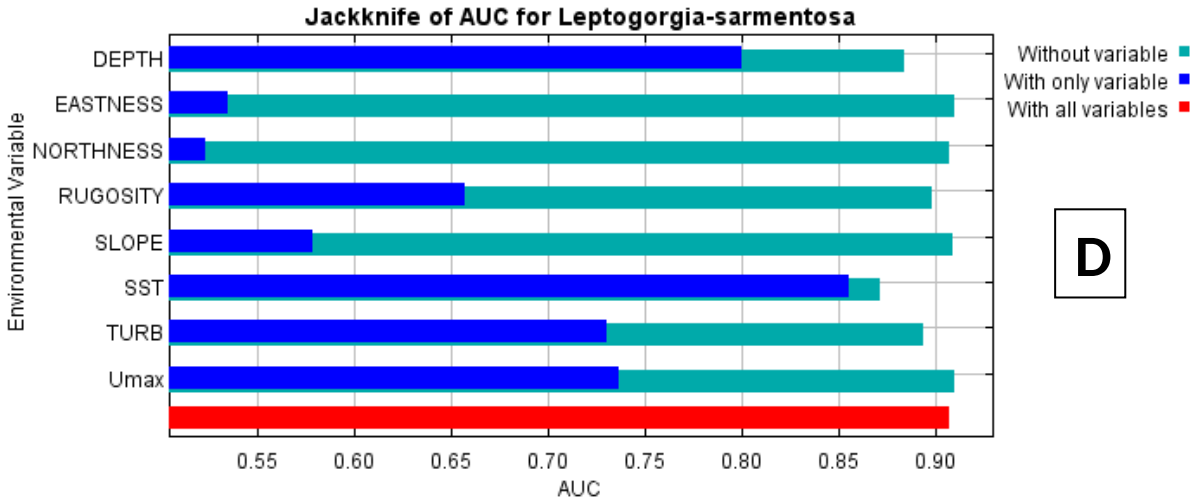

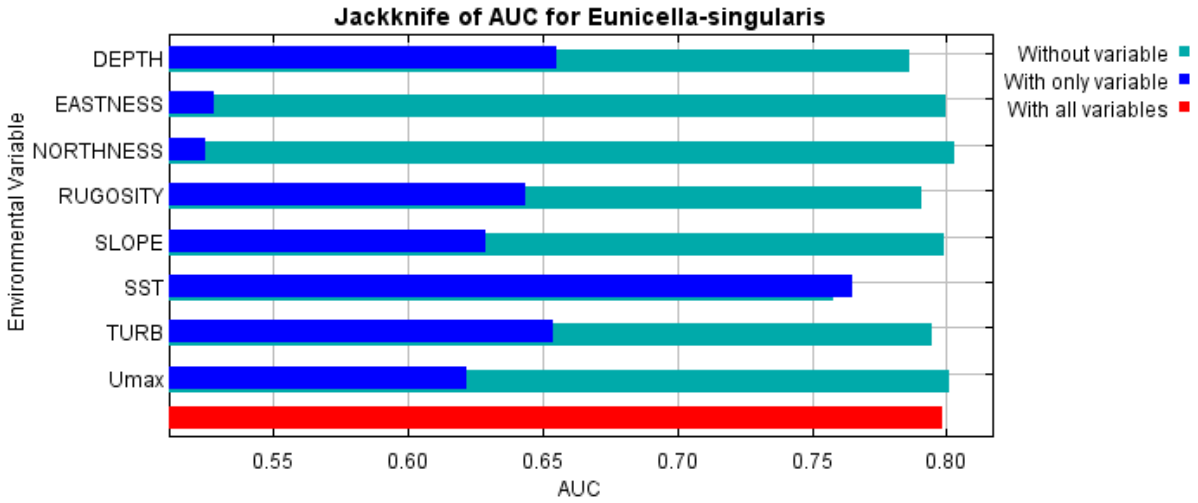

Fig S6: Jackknife of AUC (MaxENT model) Modeling with all predictors without geographical predictors (Latitude / Longitude). **A**: *C. rubrum*, **B**: *P.clavata*, **C**: *E. cavolini*, **D**: *E.singularis*, **E**: *L.*

sarmentosa. Without variable (light blue), with only variable (blue), with all variables (red). Variable is the same as predictor.

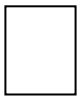

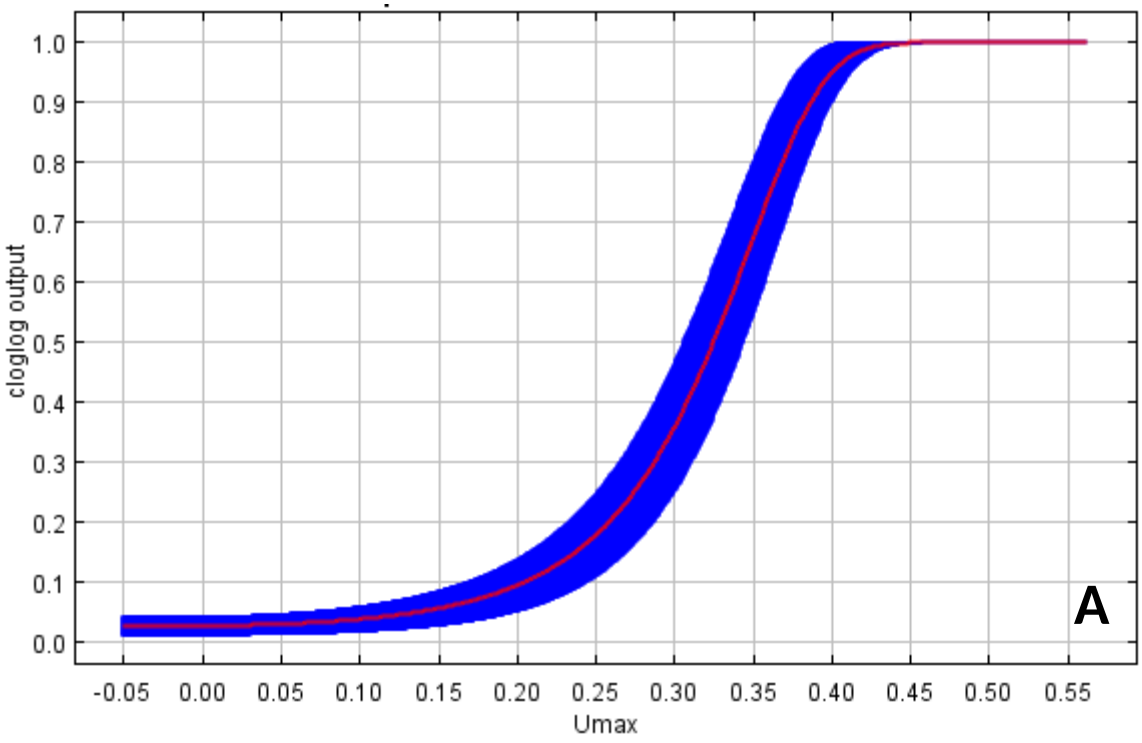
cloglog output
1.0
0.9
0.8
0.7
0.6
0.5
0.4
0.3
0.2
0.1
0.0
-0.05
0.00
0.05
0.10
0.15
0.20
0.25
0.30
0.35
0.40
0.45
0.50
0.55
Umax
A

B

Figure S7 : Response curves for the two significant predictors in the Maxent model for habitat suitability of *C. rubrum*: **A**: Maximinum flow speed on the seabed (Umax) , **B**: Turbidity. The red lines indicate the mean values, while blue areas the standard deviation limits, resulting from 5 cross-validation model runs in cloglog output.

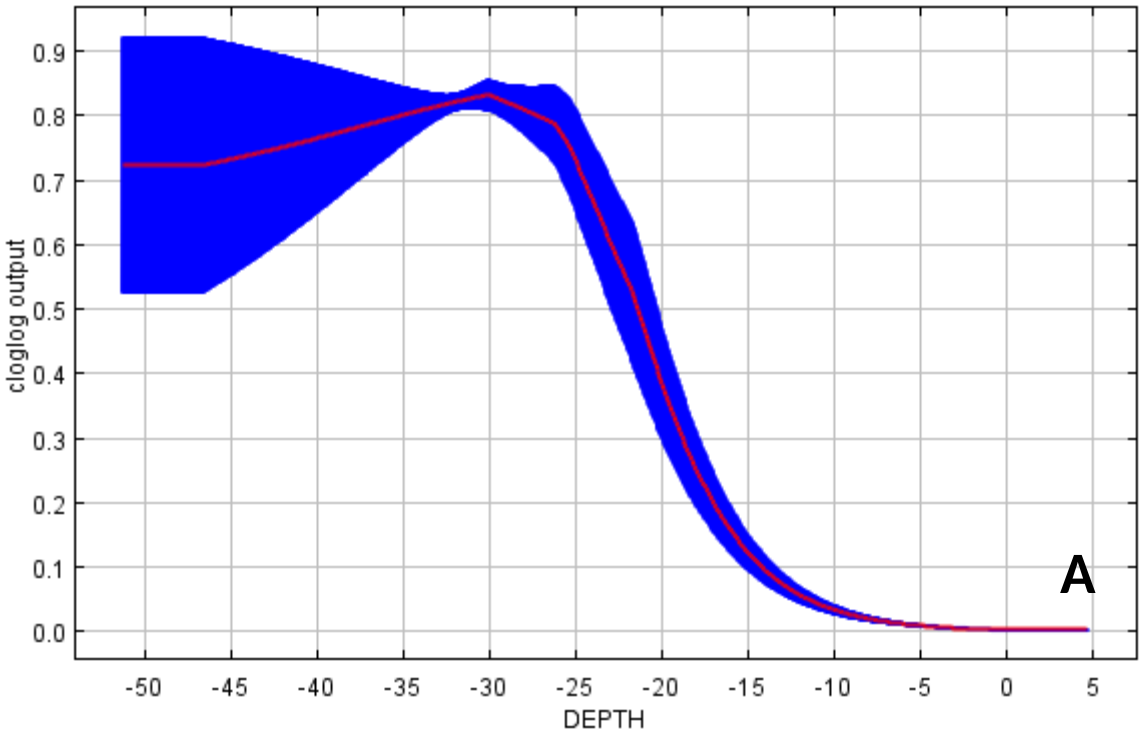
cloglog output
0.9
0.8
0.7
0.6
0.5
0.4
0.3
0.2
0.1
0.0
-50
-45
-40
-35
-30
-25
-20
-15
-10
-5
0
5
DEPTH
A

B

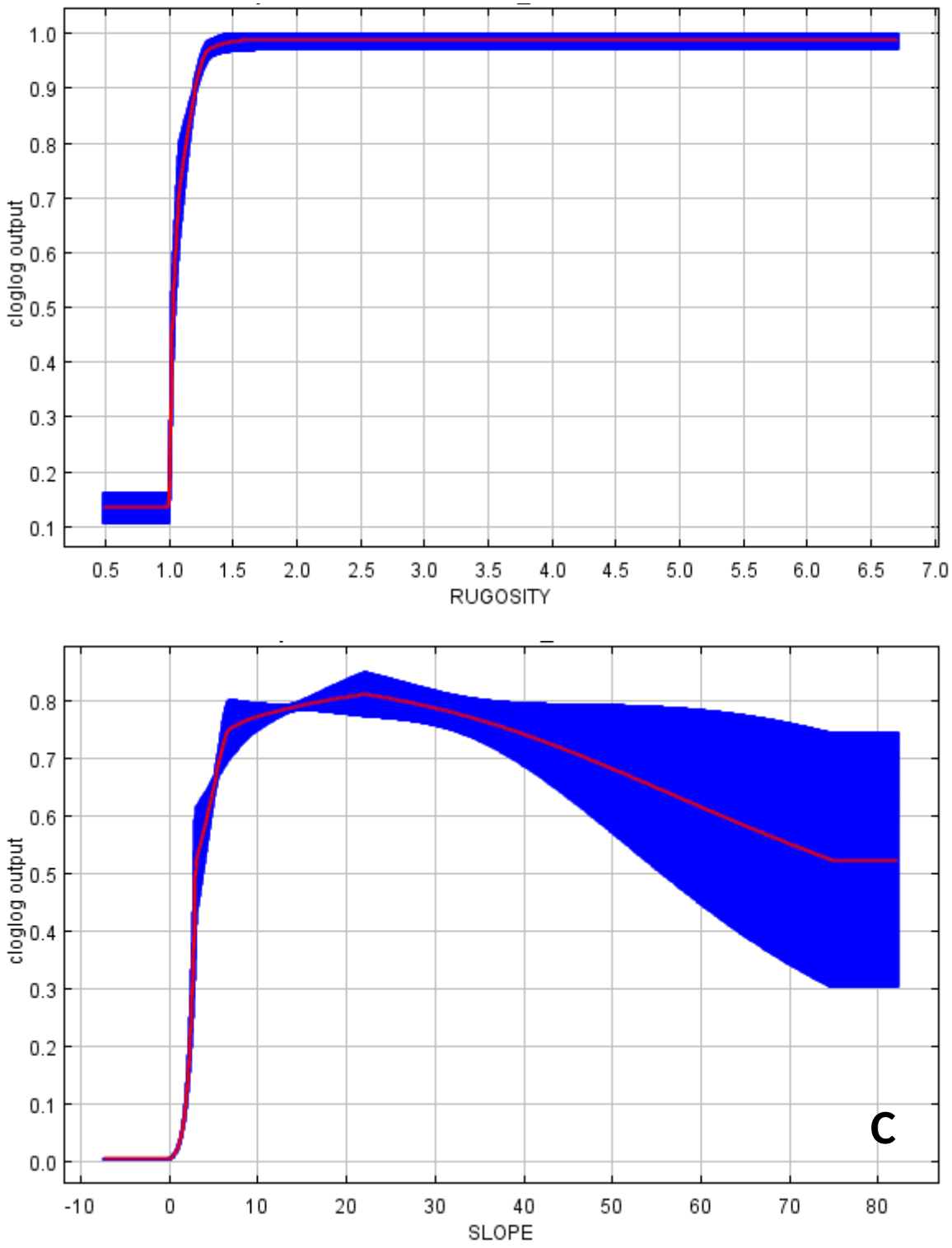

Figure S8: Response curves for the three significant predictors in the Maxent model for habitat suitability of *P.clavata*. **A**: Depth , **B**: Rugosity, **C**: Slope. The red lines indicate the mean values, while blue areas the standard deviation limits, resulting from 5 cross-validation model runs in cloglog output.

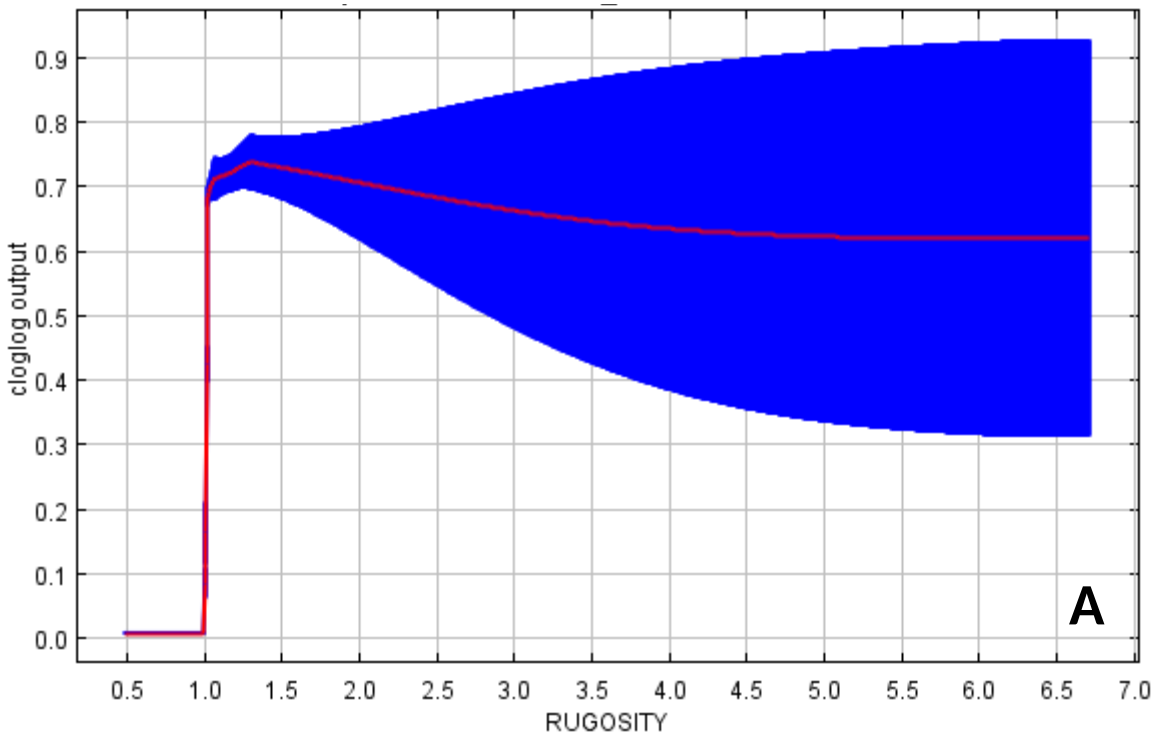
cloglog output
0.0
0.1
0.2
0.3
0.4
0.5
0.6
0.7
0.8
0.9
0.5
1.0
1.5
2.0
2.5
3.0
3.5
4.0
4.5
5.0
5.5
6.0
6.5
7.0
RUGOSITY
A

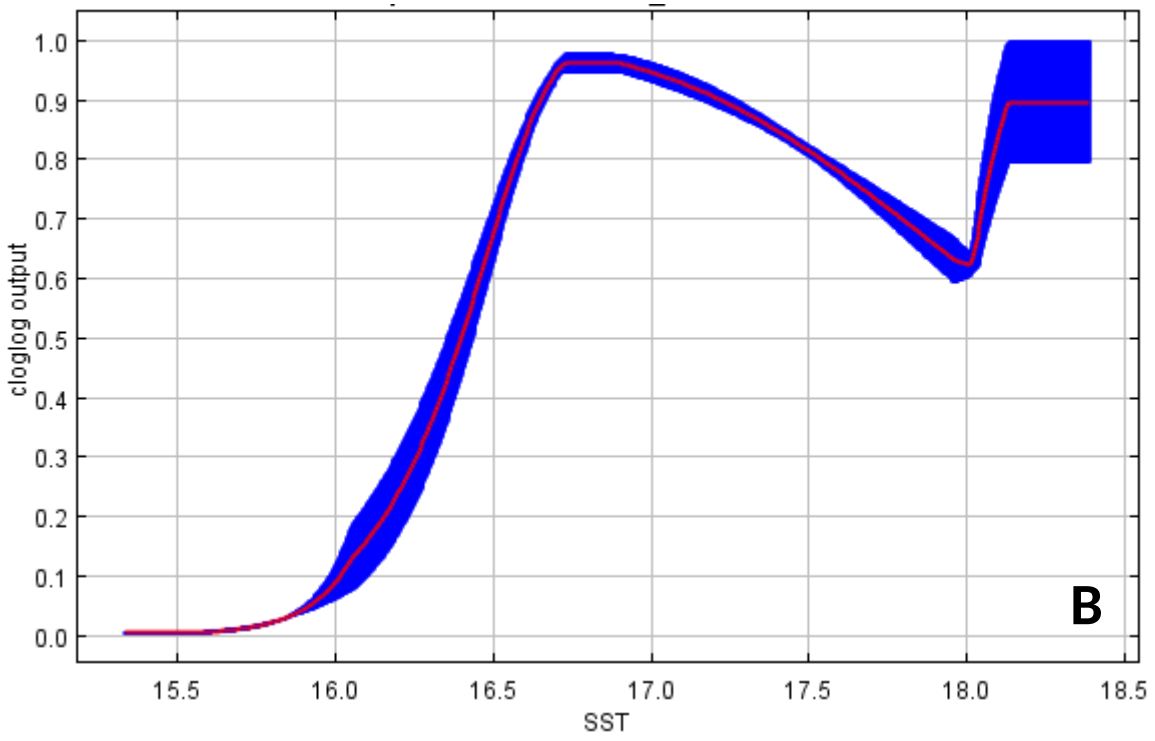
cloglog output
0.0
0.1
0.2
0.3
0.4
0.5
0.6
0.7
0.8
0.9
1.0
15.5
16.0
16.5
17.0
17.5
18.0
18.5
SST
B

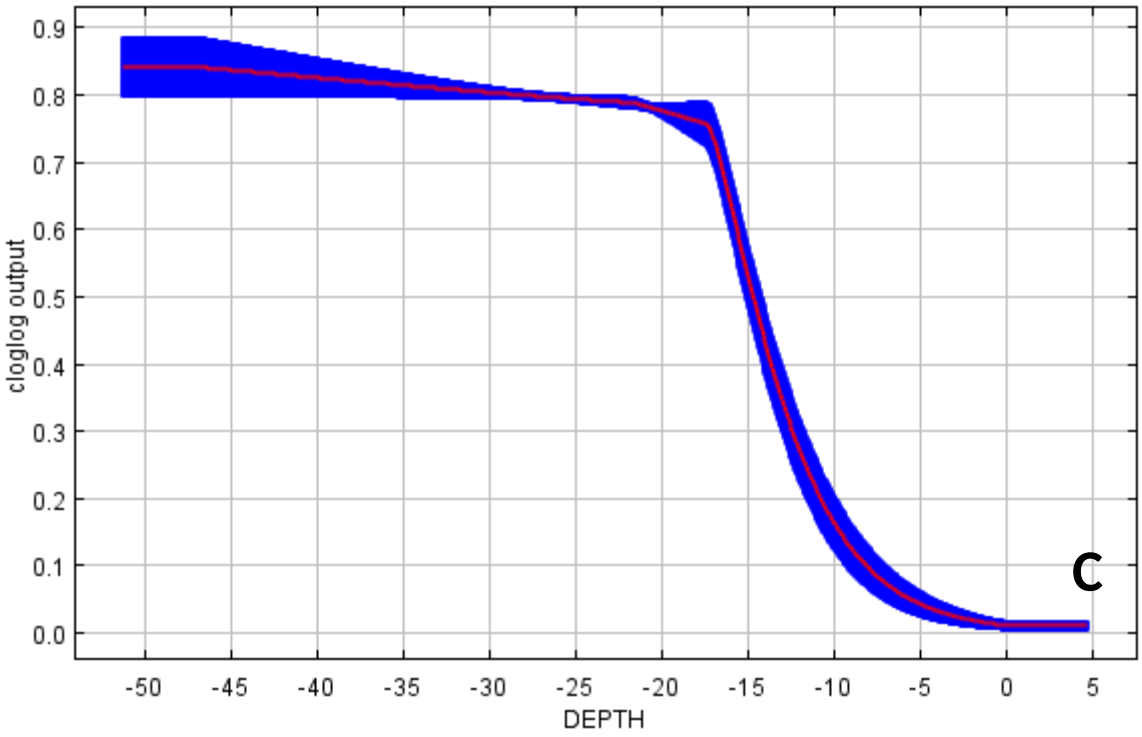

Figure S9: Response curves for the three significant predictors in the Maxent model for habitat suitability of *E.cavolini*. **A**: Rugosity, **B**: Sea Surface Temperature (SST), **C**: Depth. The red lines indicate the mean values, while blue areas the standard deviation limits, resulting from 5 cross-validation model runs in cloglog output.

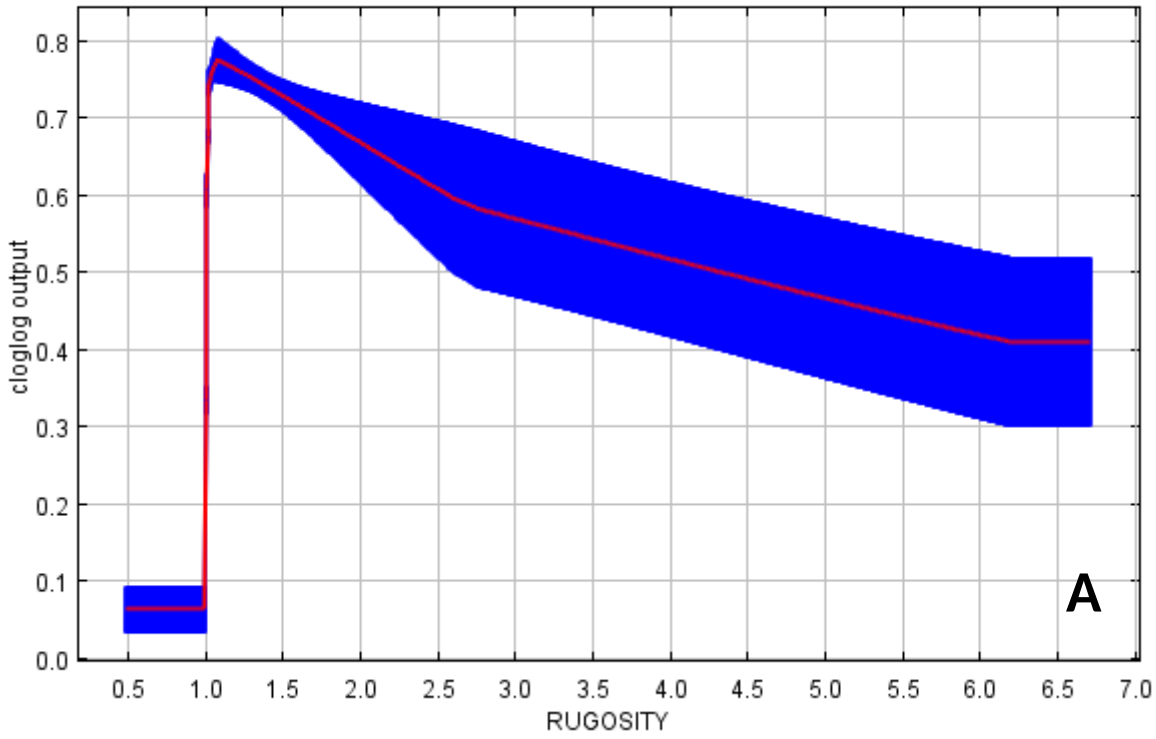
cloglog output
0.0
0.1
0.2
0.3
0.4
0.5
0.6
0.7
0.8
0.5
1.0
1.5
2.0
2.5
3.0
3.5
4.0
4.5
5.0
5.5
6.0
6.5
7.0
RUGOSITY
A

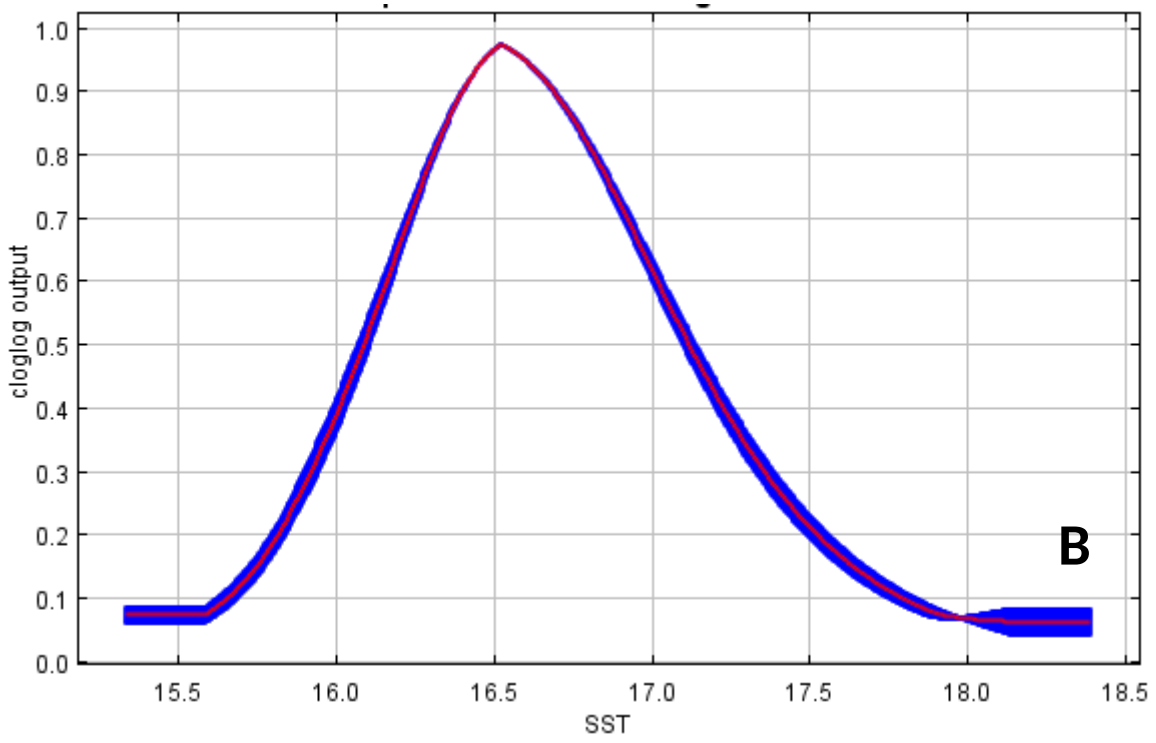
cloglog output
0.0
0.1
0.2
0.3
0.4
0.5
0.6
0.7
0.8
0.9
1.0
15.5
16.0
16.5
17.0
17.5
18.0
18.5
SST
B

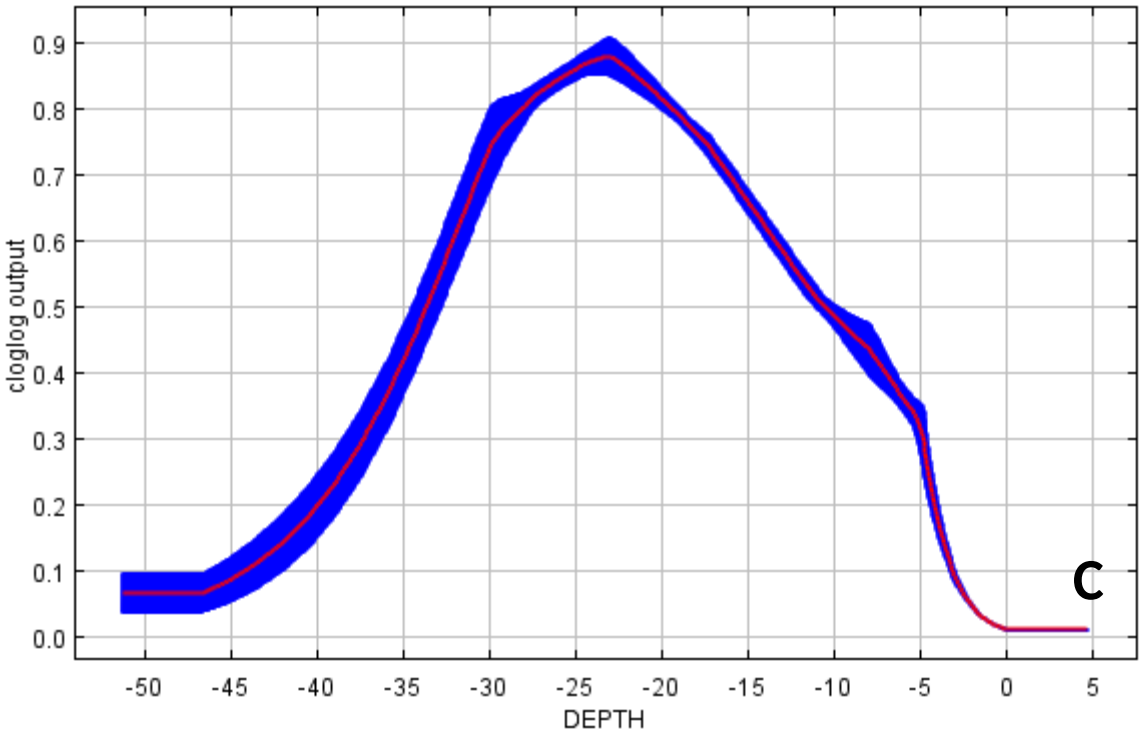

Figure S10: Response curves for the three significant predictors in the Maxent model for habitat suitability of *E.singularis*. **A**: Rugosity, **B**: Sea Surface Temperature (SST), **C**: Depth. The red lines indicate the mean values, while blue areas the standard deviation limits, resulting from 5 cross-validation model runs in cloglog output.

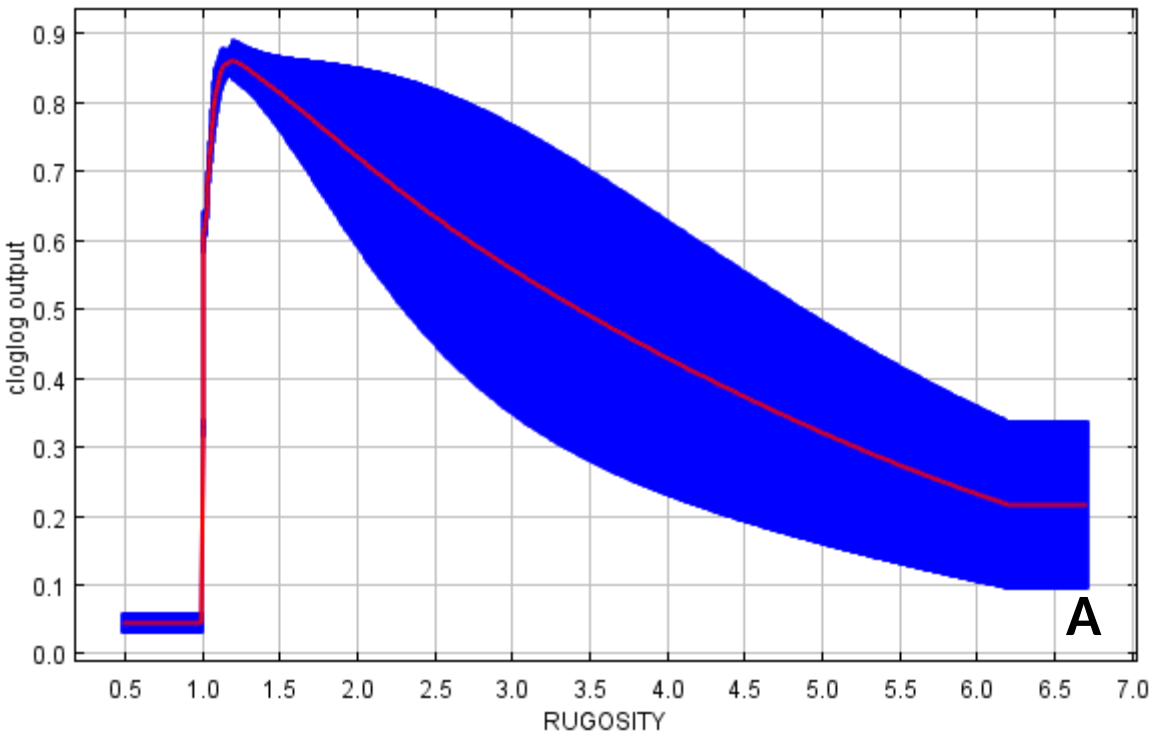

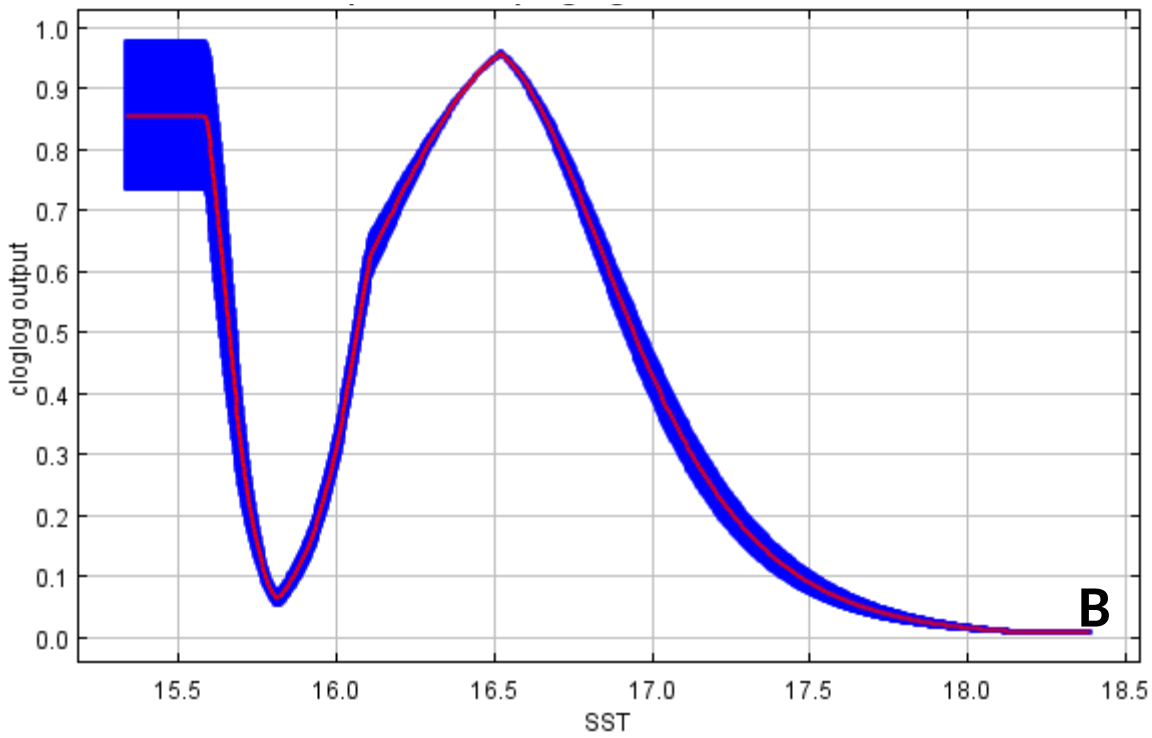
cloglog output
1.0
0.9
0.8
0.7
0.6
0.5
0.4
0.3
0.2
0.1
0.0
15.5
16.0
16.5
17.0
17.5
18.0
18.5
SST
B

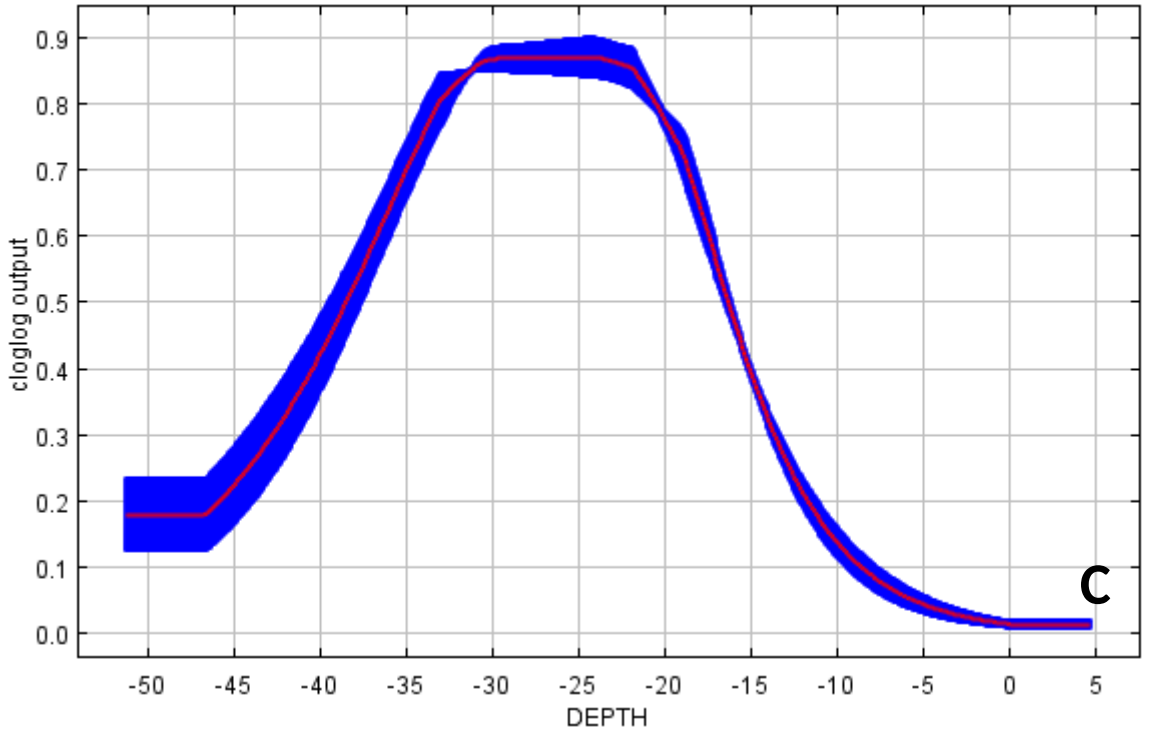
cloglog output
0.9
0.8
0.7
0.6
0.5
0.4
0.3
0.2
0.1
0.0
-50
-45
-40
-35
-30
-25
-20
-15
-10
-5
0
5
DEPTH
C

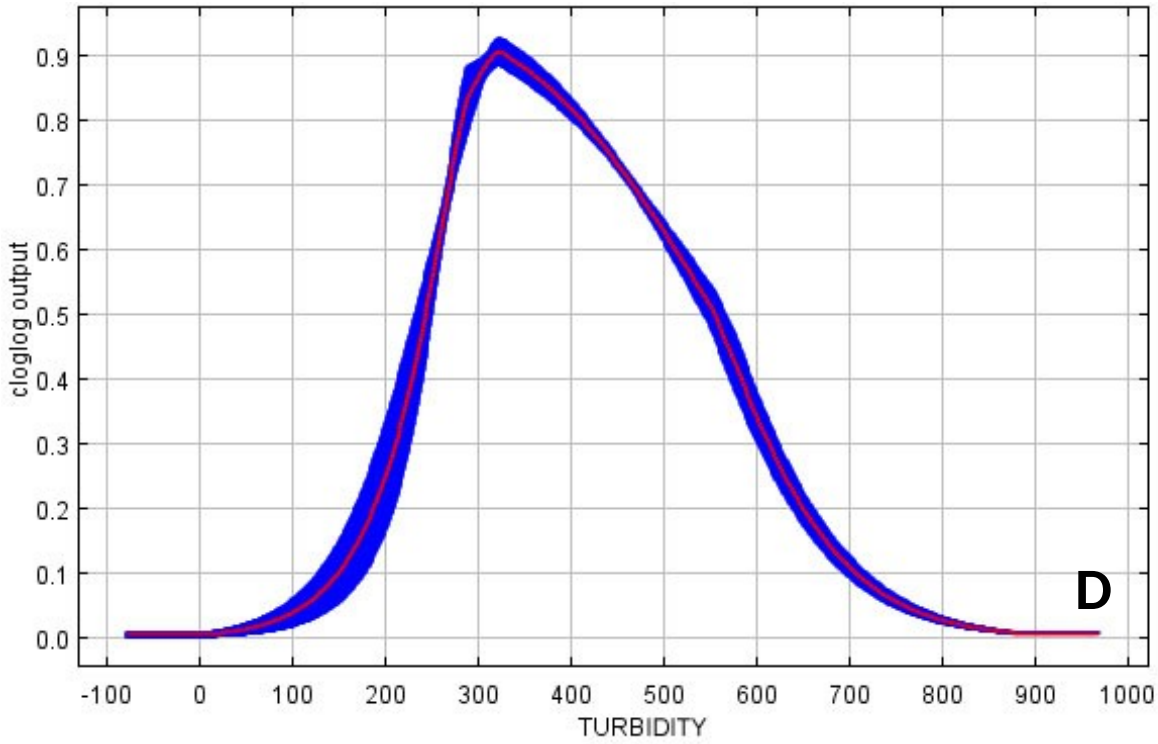

Figure S11: Response curves for the four significant predictors in the Maxent model for habitat suitability of *L. sarmentosa*. **A**: Rugosity, **B**: Sea Surface Temperature (SST), **C**: Depth, **D**: Turbidity. The red lines indicate the mean values, while blue areas the standard deviation limits, resulting from 5 cross-validation model runs in cloglog output.

Table S1: Result of model for each species with all predictors with geographical predictors (Lat / Lon). Percent contribution and permutation importance

	AUC	**Variables**	**Percent contribution (%)**	**Permutation importance (%)**
C. rubrum	0.9628	Umax	58.5	14.3
		Latitude	25.1	0
		Turbidity	10.8	81.9
P. clavata	0.9731	Depth	37.5	47.7
		Rugosity	32.2	15.5
		Slope	14.3	19
E. cavolini	0.9491	Longitude	34	0.2
		Rugosity	32.7	39.8
		Depth	22.8	13.1
		Latitude	6.9	27
E. singularis	0.8133	Latitude	52.2	35.7
		Depth	11.1	23.5
		Longitude	10	11.8
L. sarmentosa	0.9731	Longitude	46.7	24.3
		Latitude	25.1	46.2
		Turbidity	8.1	15.5

(1)

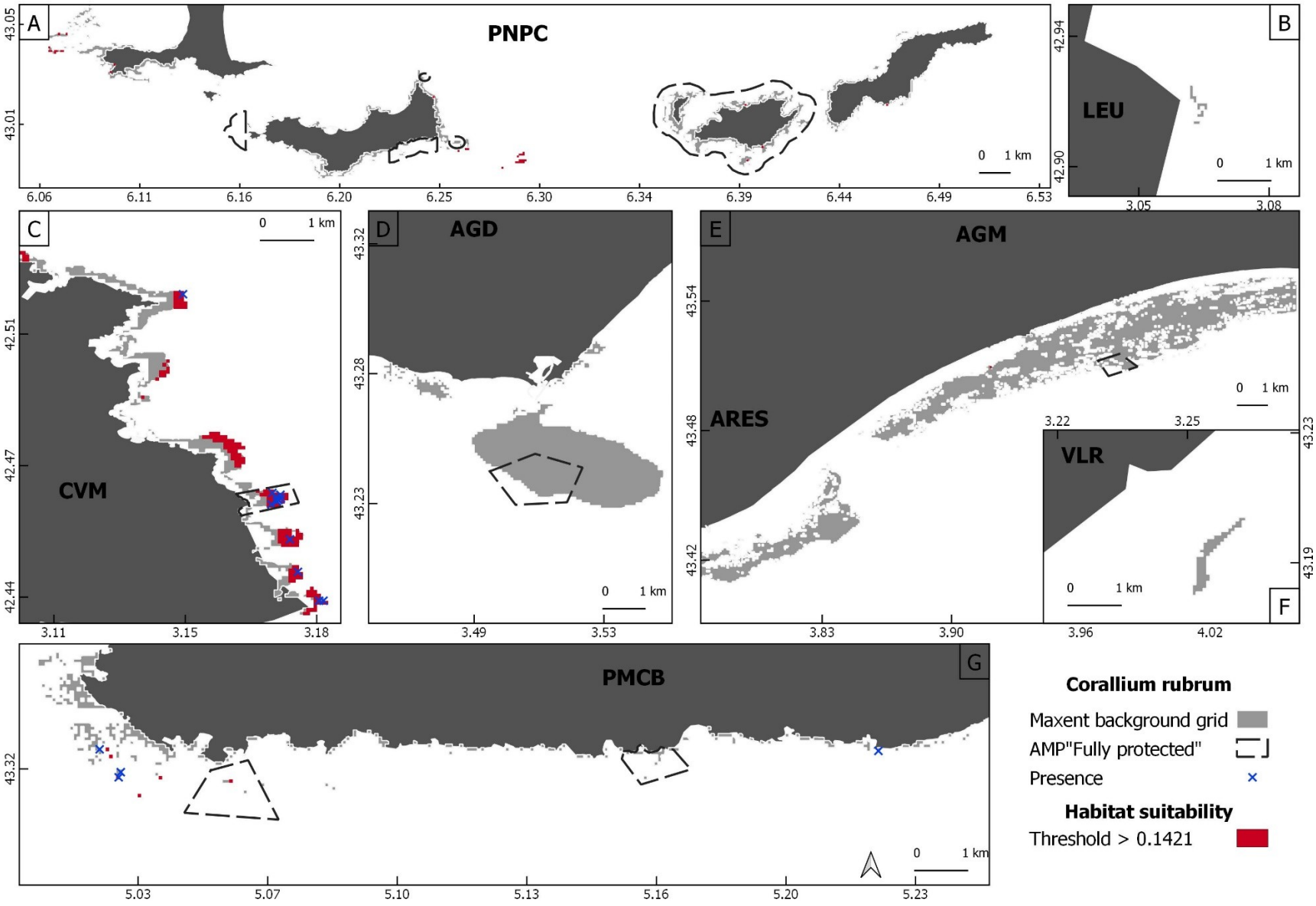
A
PNPC
B
LEU
C
CVM
D
AGD
E
AGM
ARES
F
VLR
G
PMCB
0 1 km
Corallium rubrum
Maxent background grid
AMP"Fully protected"
Presence
Habitat suitability
Threshold > 0.1421

(2)

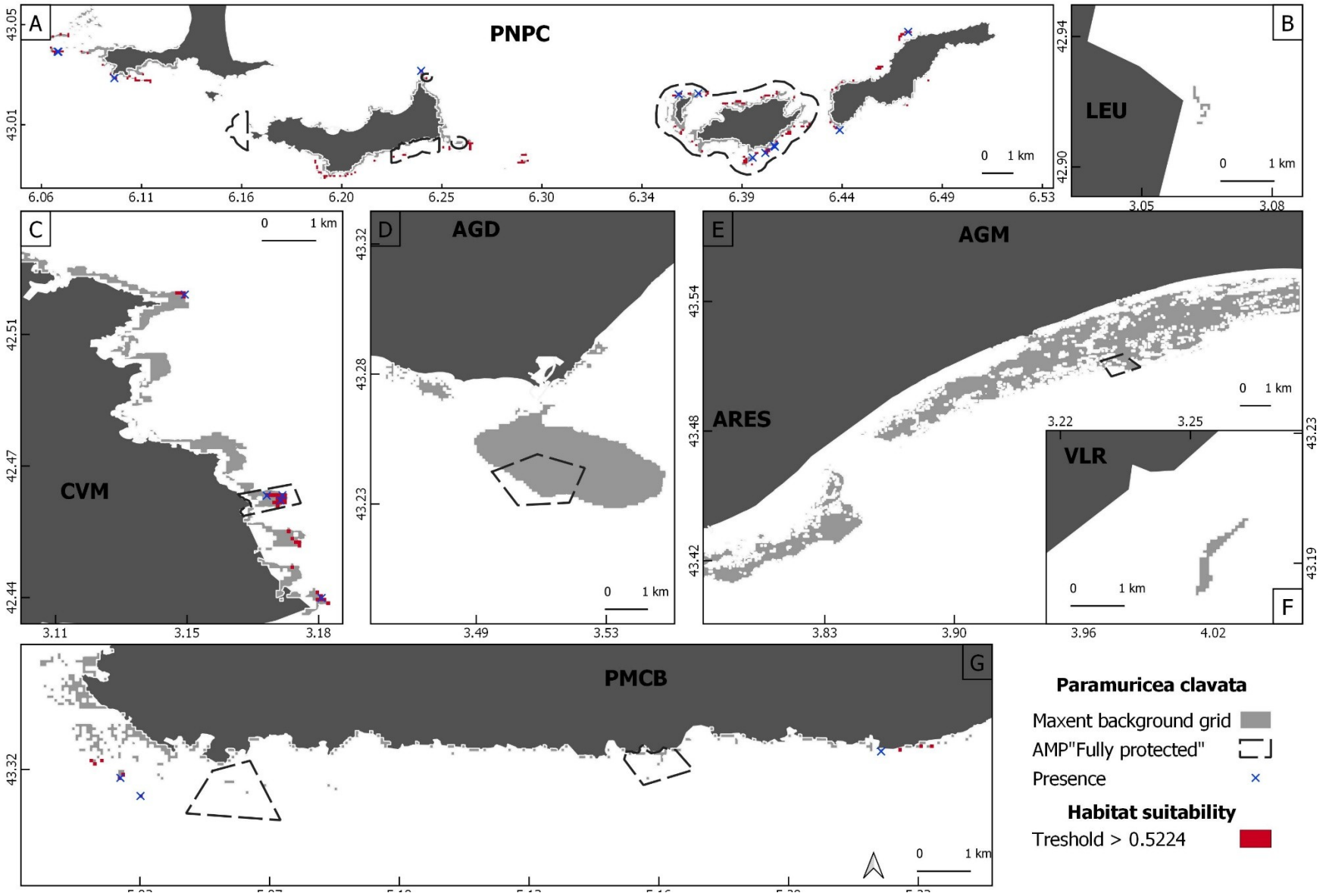
A
PNPC
B
LEU
C
CVM
D
AGD
E
AGM
ARES
F
VLR
G
PMCB
0 1 km
Paramuricea clavata
Maxent background grid
AMP"Fully protected"
Presence
Habitat suitability
Treshold > 0.5224

(3)

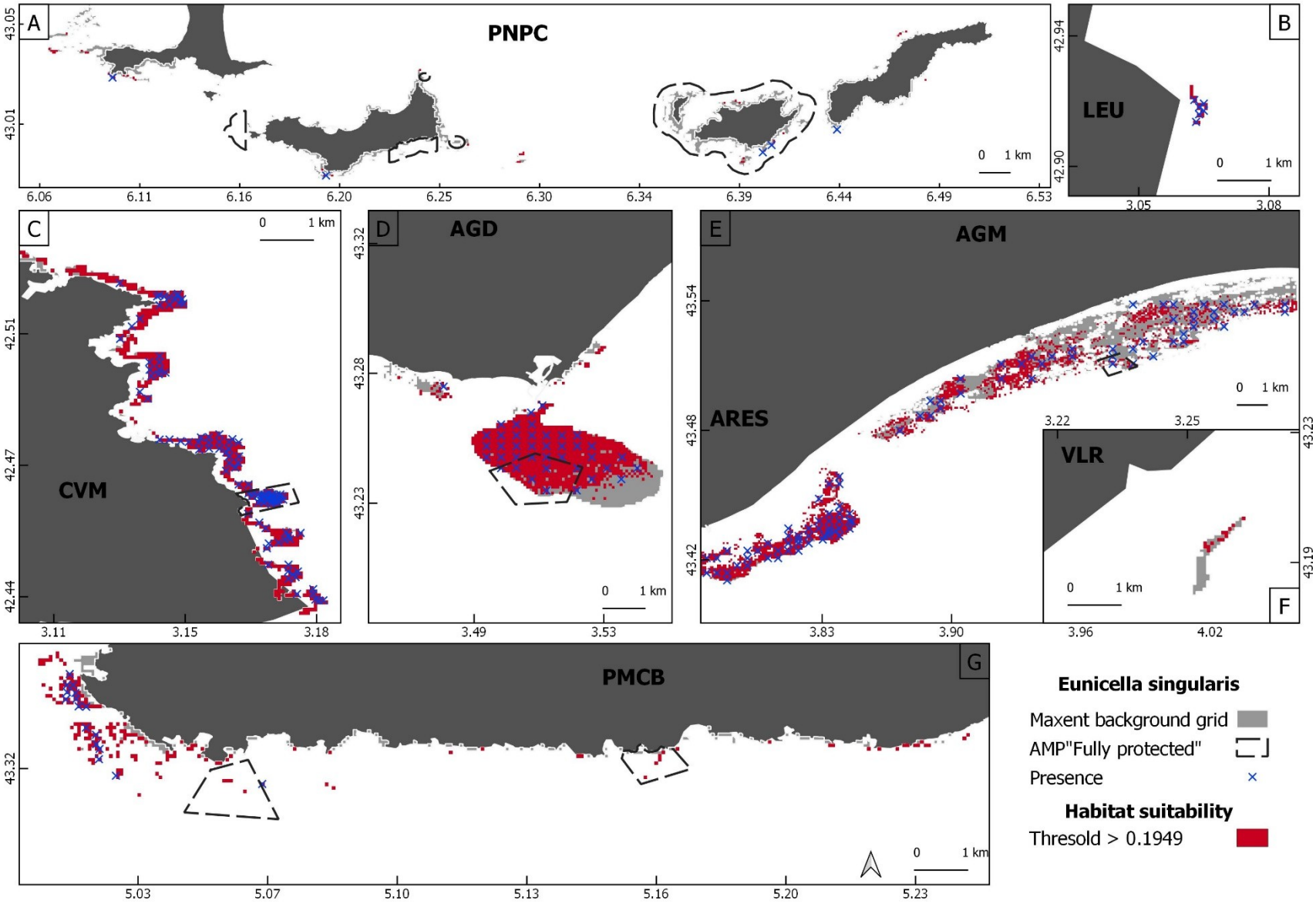
A
PNPC
B
LEU
C
CVM
D
AGD
E
AGM
ARES
F
VLR
G
PMCB
0 1 km
Eunicella singularis
Maxent background grid
AMP"Fully protected"
Presence
Habitat suitability
Thresold > 0.1949

(4)

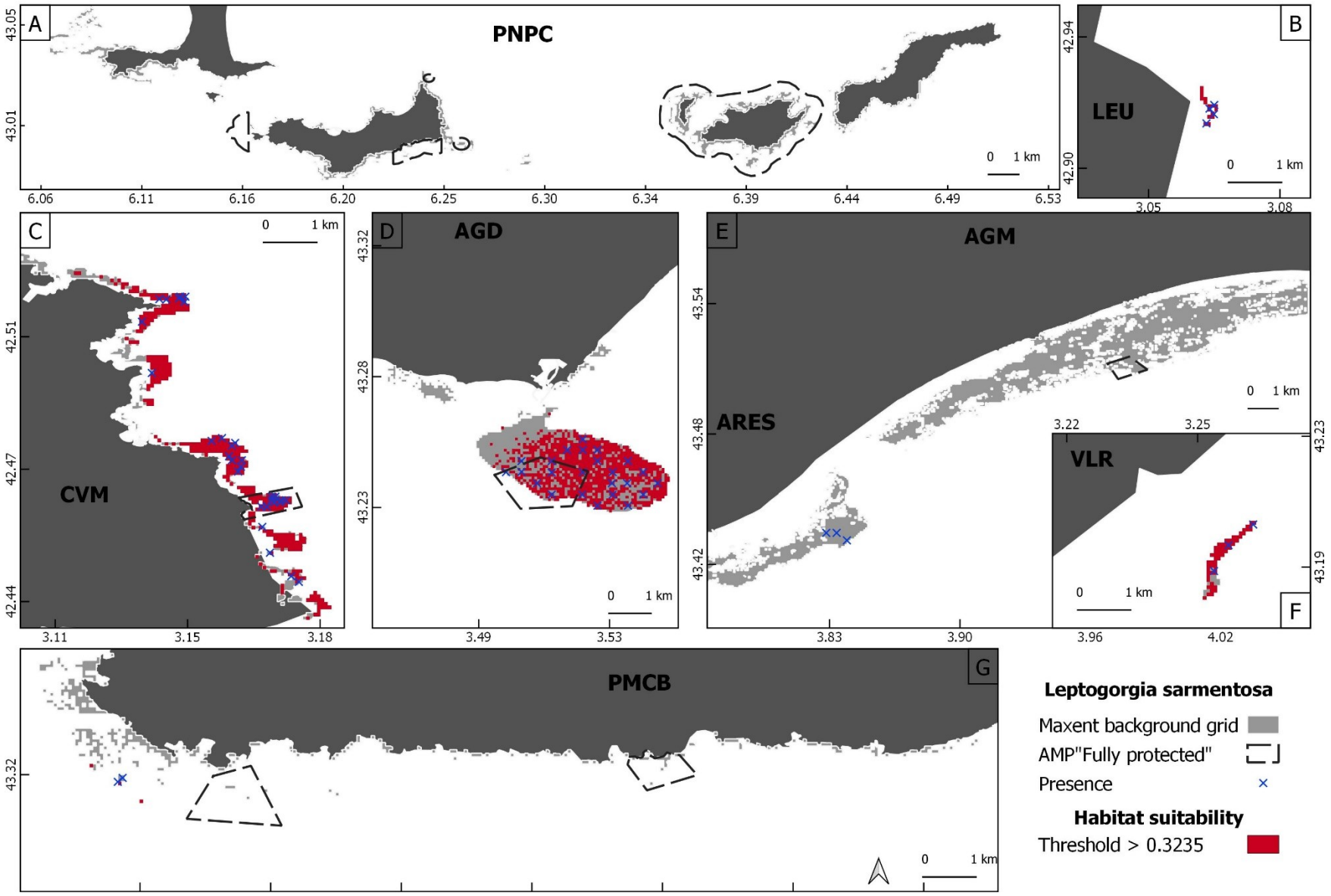
A
PNPC
B
LEU
C
CVM
D
AGD
E
AGM
ARES
F
VLR
G
PMCB
0 1 km
Leptogorgia sarmentosa
Maxent background grid
AMP"Fully protected"
Presence
Habitat suitability
Threshold > 0.3235

Figure S12: Presence location (blue cross) and a regional habitat suitability model maps predicted using maximum entropy (MaxEnt) with all predictors with geographical predictors (Latitude / Longitude) (Grid red). The habitat suitability model map was calculated by applying a threshold value to obtain binary maps (0-1) from Cloglog output. **A** close up PNPC, **B** close up LEU, **C** close up CVM, **D** close up AGD, E close up AGM and ARES, F close up VLR, G close up PMCB. Maps for : **(1)** *C.rubrum*, **(2)** *P. clavata*, **(3)** *E. singularis*,**(4)** *L. sarmentosa*.

Figures

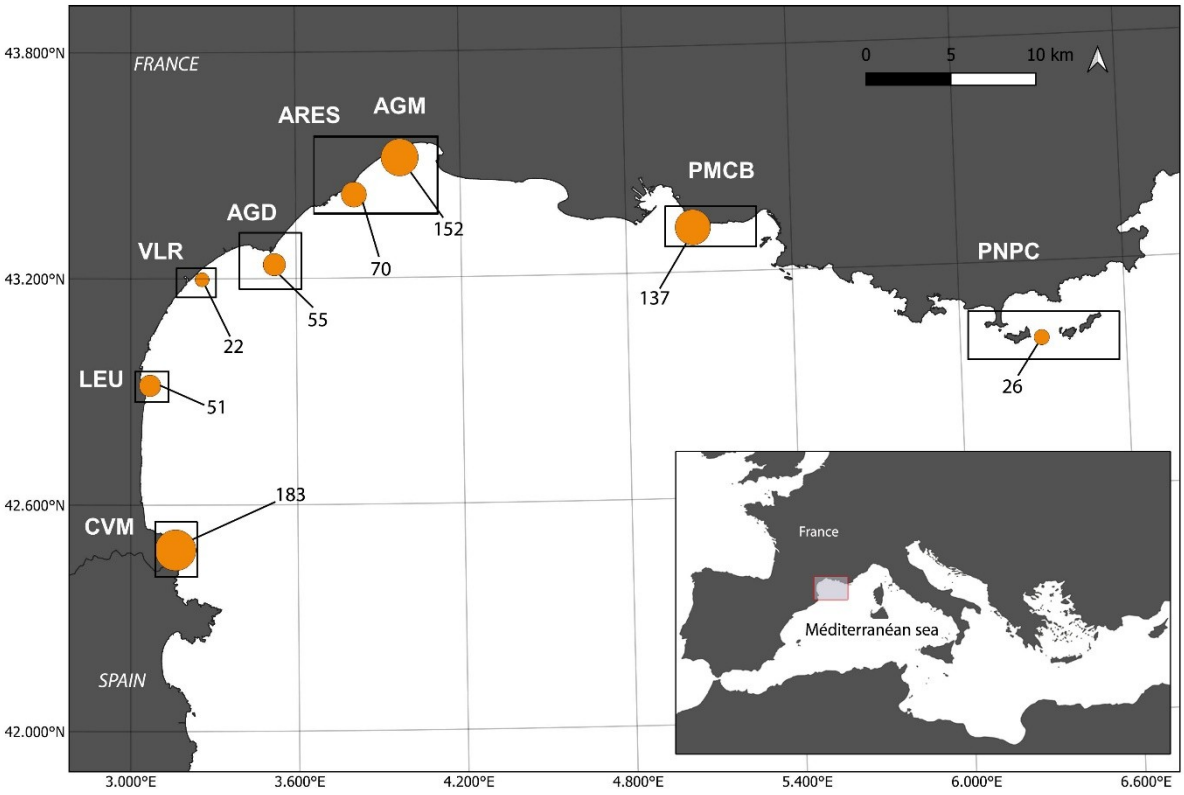

Figure 1: Map displaying the number of sampling locations in each of the eight sites of the NW Mediterranean Sea. Black rectangles highlight the sampled sites. The orange circles represent the number of sampling points at each site.

(1)

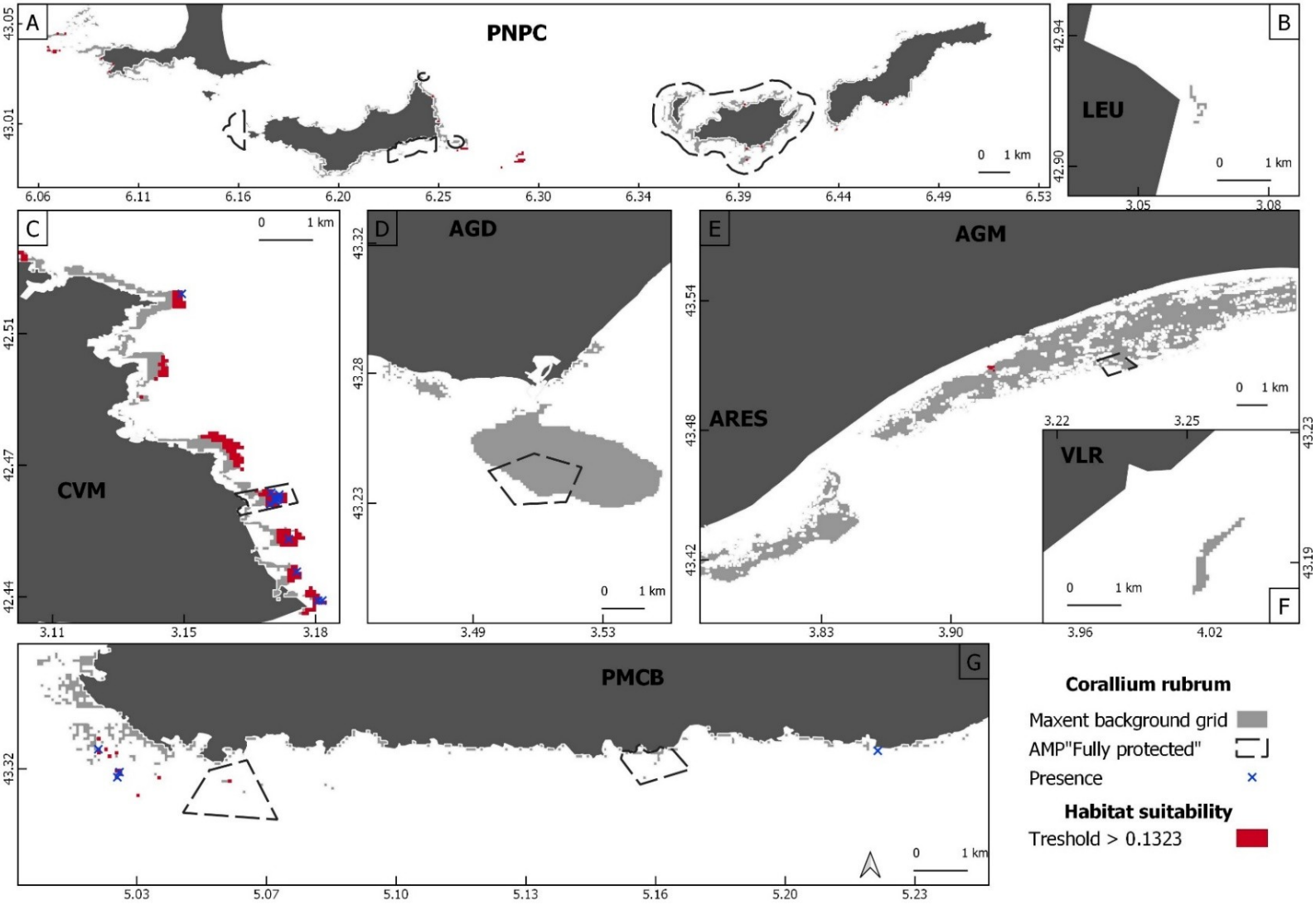
A
PNPC
B
LEU
C
CVM
D
AGD
E
AGM
ARES
F
VLR
G
PMCB
0 1 km
Corallium rubrum
Maxent background grid
AMP"Fully protected"
Presence
Habitat suitability
Treshold > 0.1323

(2)

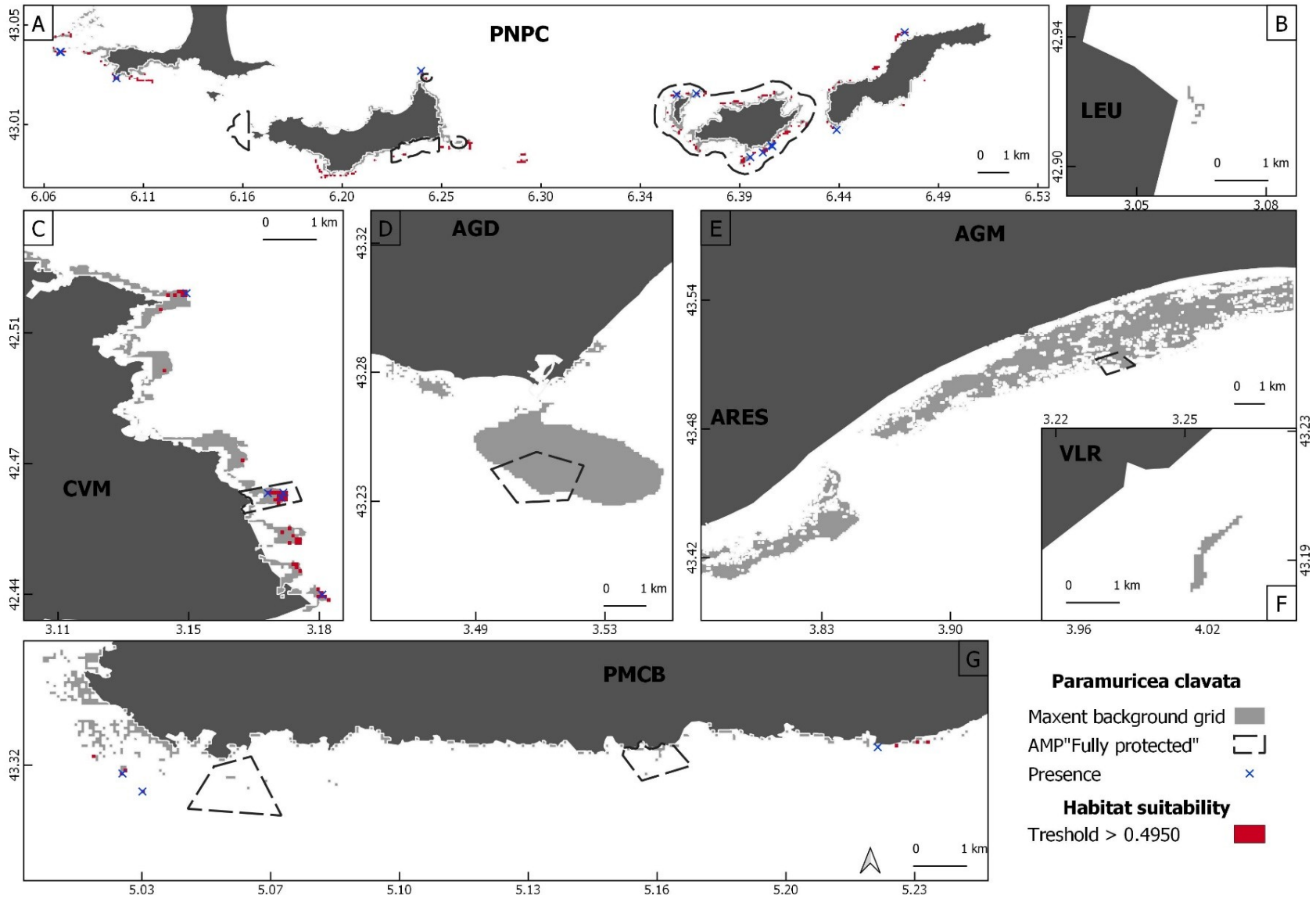
A
PNPC
B
LEU
C
CVM
D
AGD
E
AGM
ARES
F
VLR
G
PMCB
0 1 km
Paramuricea clavata
Maxent background grid
AMP"Fully protected"
Presence
Habitat suitability
Treshold > 0.4950

(3)

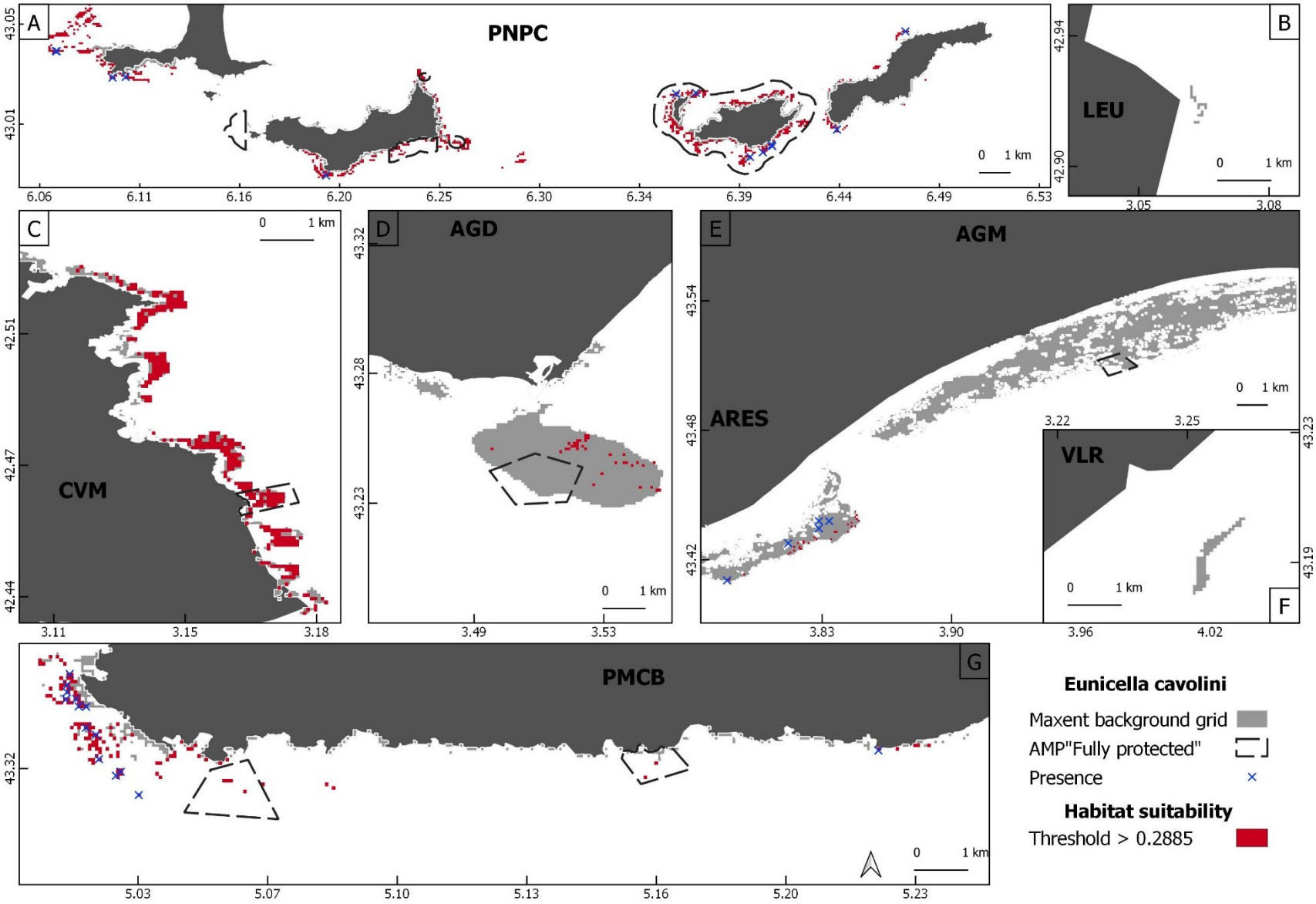
A
PNPC
B
LEU
C
CVM
D
AGD
E
AGM
ARES
F
VLR
G
PMCB
0 1 km
Eunicella cavolini
Maxent background grid
AMP"Fully protected"
Presence
Habitat suitability
Threshold > 0.2885

(4)

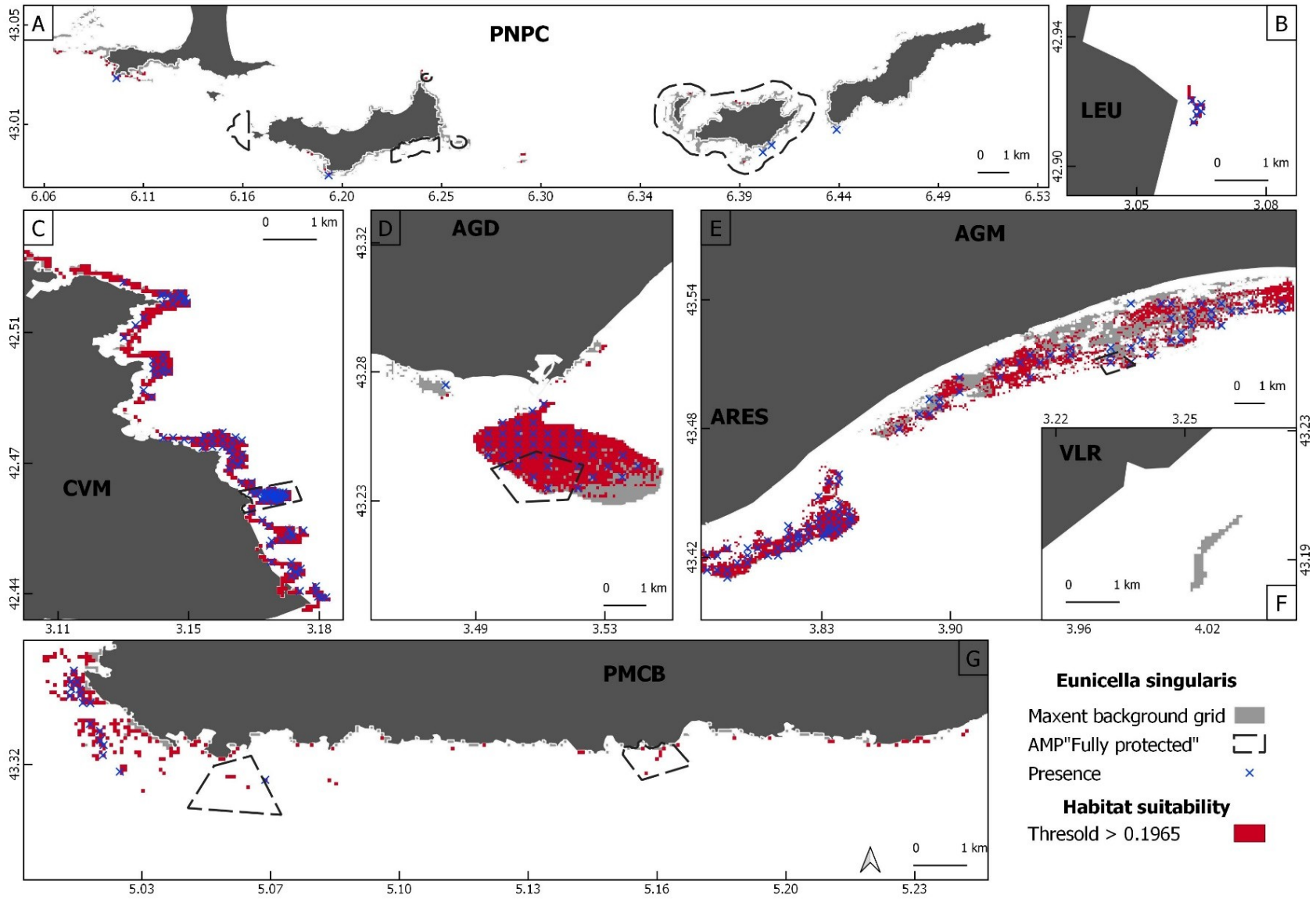
A
PNPC
B
LEU
C
CVM
D
AGD
E
AGM
ARES
VLR
F
G
PMCB
0 1 km
Eunicella singularis
Maxent background grid
AMP"Fully protected"
Presence
Habitat suitability
Thresold > 0.1965

(5)

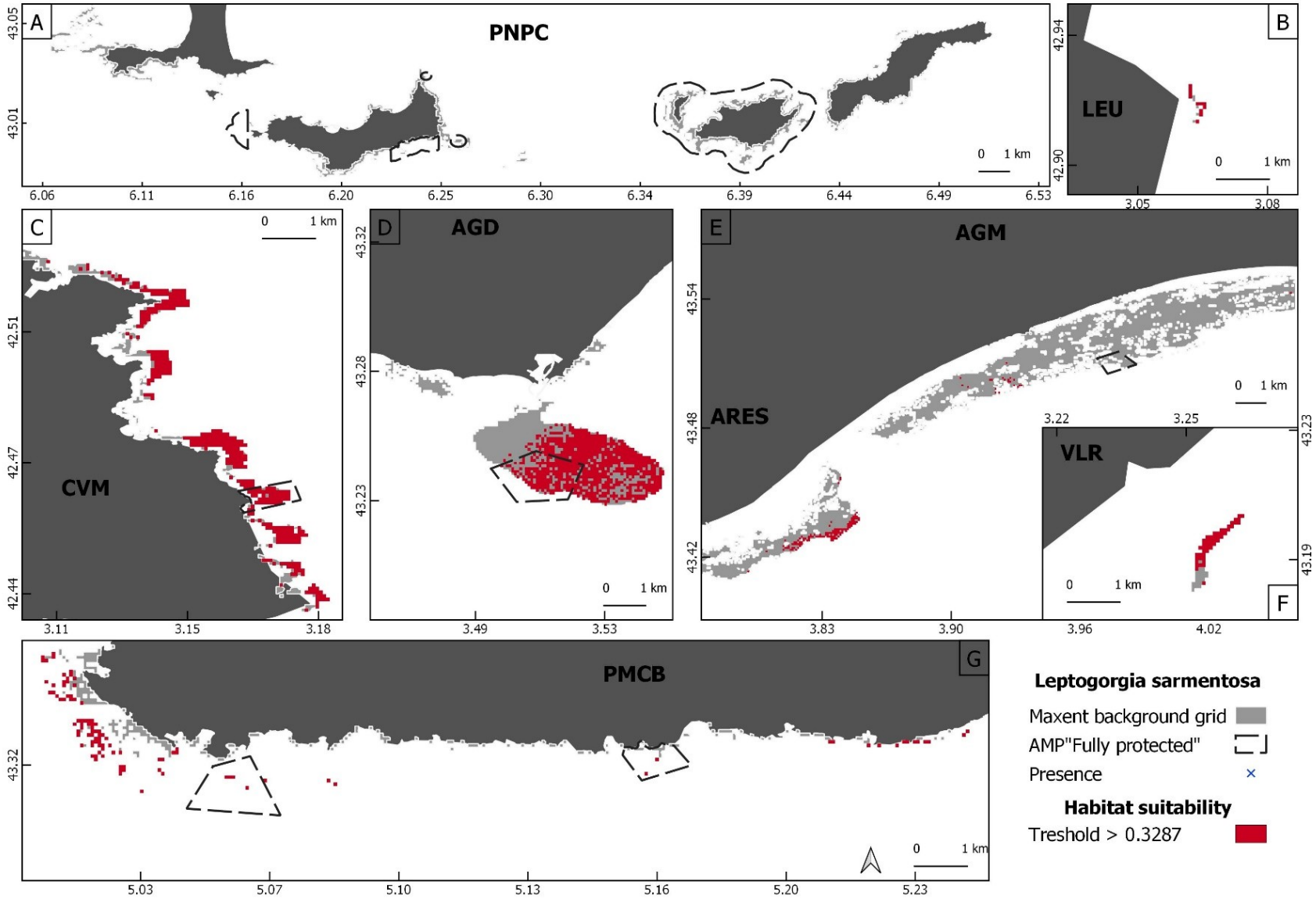
A
PNPC
B
LEU
C
CVM
D
AGD
E
AGM
ARES
F
VLR
G
PMCB
0 1 km
Leptogorgia sarmentosa
Maxent background grid
AMP"Fully protected"
Presence
Habitat suitability
Treshold > 0.3287

Figure 2: Presence location (Blue cross) and a regional habitat suitability model maps predicted using maximum entropy (MaxEnt) with all predictors without geographical predictors (Latitude / Longitude) (Grid red). The habitat suitability model map was calculated by applying a threshold value to obtain binary maps (0-1) from Cloglog output. **A** close up PNPC, **B** close up LEU, **C** close up CVM, **D** close up AGD, E close up AGM and ARES, F close up VLR, G close up PMCB. Maps for : **(1)** *C.rubrum*, **(2)** *P. clavata*,**(3)** *E. cavolini*, **(4)** *E. singularis*,**(5)** *L. sarmentosa*.

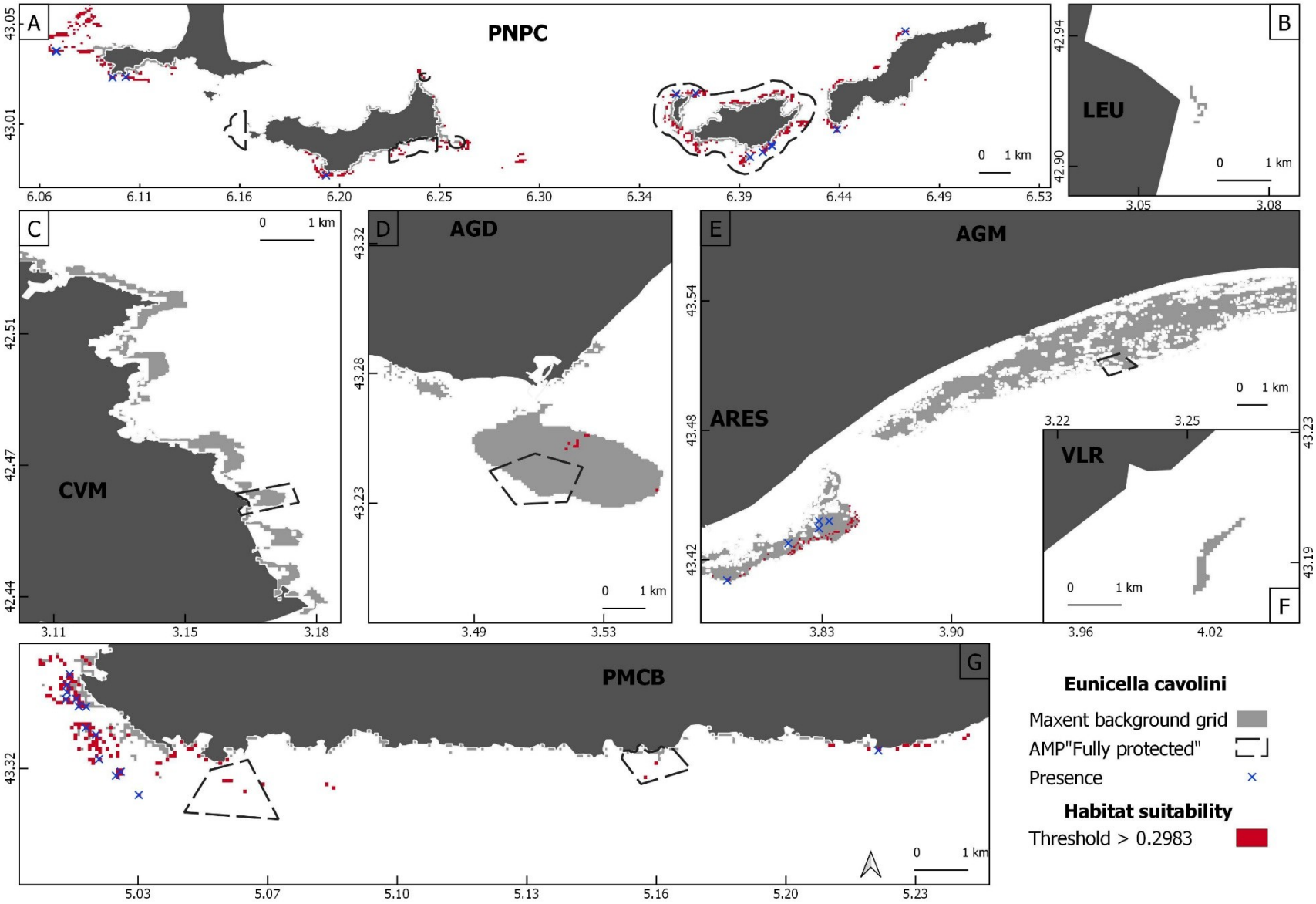
A
PNPC
B
LEU
C
CVM
D
AGD
E
AGM
ARES
F
VLR
G
PMCB
0 1 km
Eunicella cavolini
Maxent background grid
AMP"Fully protected"
Presence
Habitat suitability
Threshold > 0.2983

Figure 2a: Presence location (Blue cross) and a regional habitat suitability model maps predicted using maximum entropy (MaxEnt) for *E. cavolini* with all predictors with geographical predictors (Latitude / Longitude) (Grid red). The habitat suitability model map was calculated by applying a threshold (0.2983) to obtain binary maps (0-1) from Cloglog output. **A** close up PNPC, **B** close up LEU, **C** close up CVM, **D** close up AGD, E close up AGM and ARES, F close up VLR, G close up PMCB.

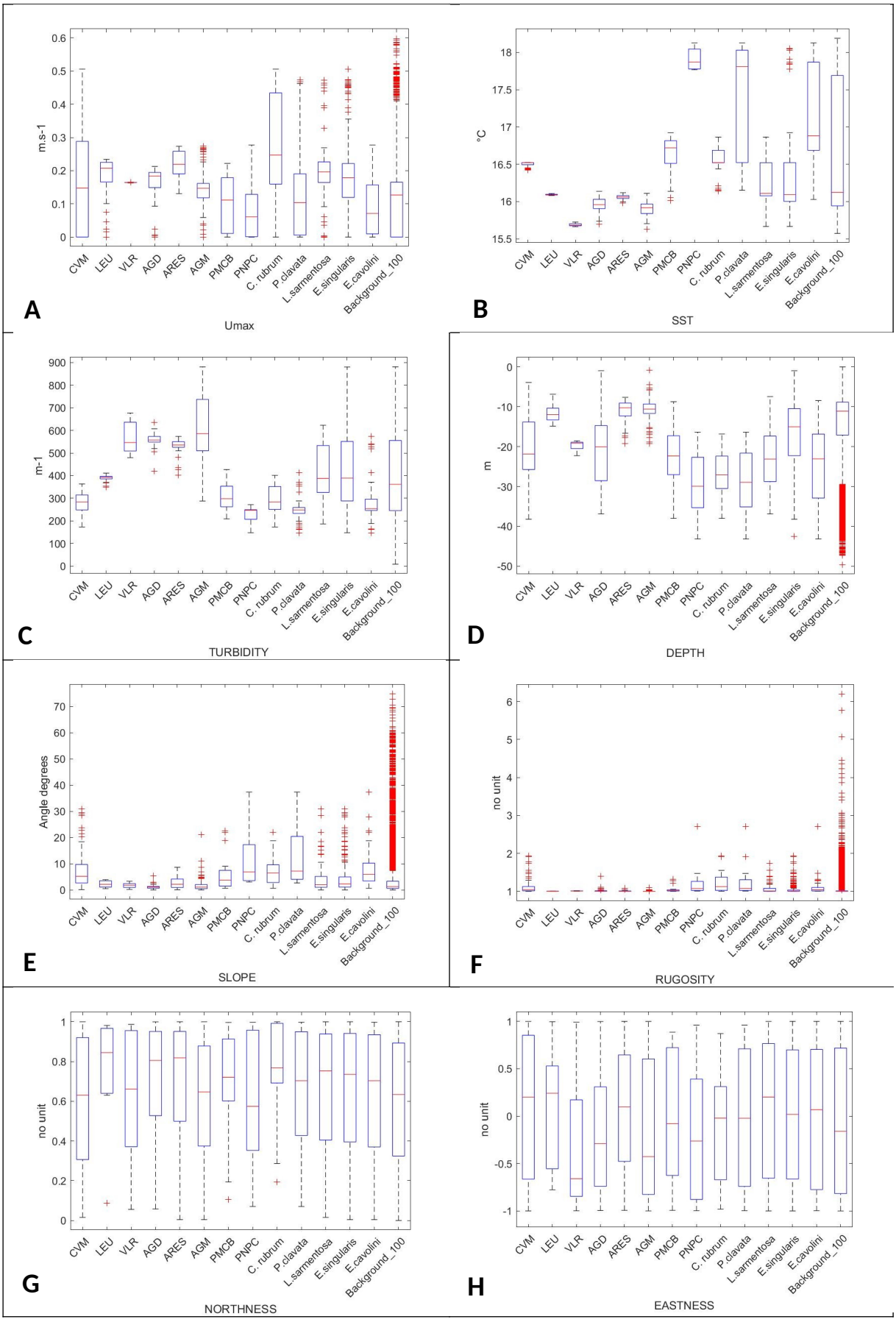
A
m.s-1
Umax
B
°C
SST
C
m-1
TURBIDITY
D
m
DEPTH
E
Angle degrees
SLOPE
F
no unit
RUGOSITY
G
no unit
NORTHNESS
H
no unit
EASTNESS
CVM
LEU
VLR
AGD
ARES
AGM
PMCB
PNPC
C. rubrum
P.clavata
L.sarmentosa
E.singularis
E.cavolini
Background_100

Figure 3: Boxplot of the 9 predictors no-correlated selected in the 8 sites (CVM, LEU, VLR, AGD, ARES, AGM, PMCB, PNPC), for all species, in all sampling (sampling), and in the background: These data are extracted in cells grid of 100 m * 100m; (A: Umax, B: SST, C: TURBIDITY, D: DEPTH, E: SLOPE, F: RUGOSITY, G: NORTHNESS, H: EASTNESS)

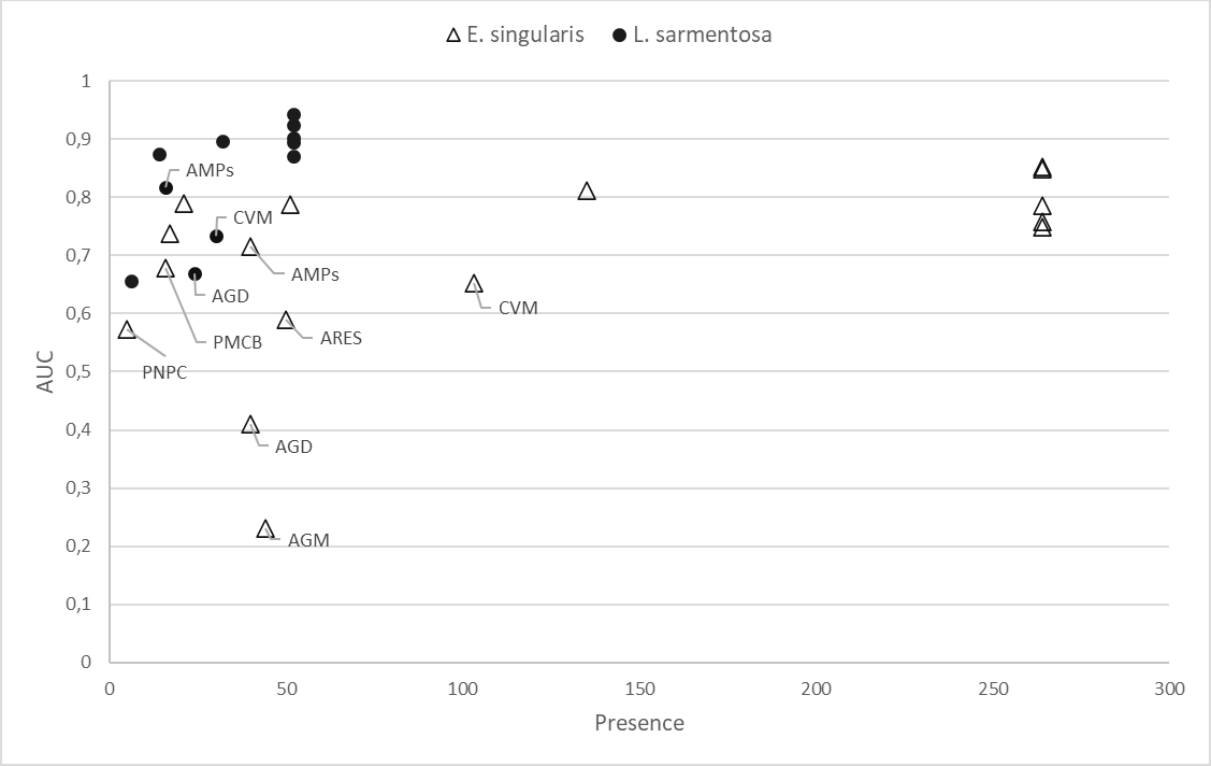

Fig 4: Assessment of the AUC for *Eunicella singularis* (white triangle) and *Leptogorgia sarmentosa* (dark cercle) varying the number of presence data (100 - 7%) where their location while keeping the full presence data in the testing dataset.

Tables

Table 1: Result of model for each species with all predictors without geographical predictors (Lat / Lon). Percent contribution and permutation importance

	Variables	Percent contribution (%)	Permutation importance (%)
C. rubrum	Umax	71.9	31.4
	Turbidity	23.1	62.6
P. clavata	Depth	36.3	46.7
	Rugosity	31.1	21.2
	Slope	14.9	16.2
E. cavolini	Rugosity	41.3	39.3
	SST	28.7	32.2
	Depth	239	20.5
E. singularis	SST	44.5	36.8
	Rugosity	20.1	18.5
	Depth	14.4	26.7
L. sarmentosa	Depth	37.8	21.8
	Rugosity	21.3	25
	SST	17.6	25.7
	Turbidity	13.5	20.4

Table 2: Results of assessment of model performance with all predictors without geographical predictors (Lat / Lon) (AUC, Accuracy, sensitivity: true positif , specificity: true absence; Italic: results for the modelling with only sampling in AMPs) (number of cells compared = 468)

	AUC test	Accuracy	Sensitivity	Specificity	TSS	Chi^2
C. rubrum	0.971(*0.994)*	0.87(*0.94)*	0.24*(0.39)*	1*(0.98)*	0.24*(0.38)*	P<0.0001
P. clavata	0.964(*0.931)*	0.92*(0.87)*	0.34*(0.22)*	1*(0.99)*	0.34*(0.22)*	P<0.0001
E. cavolini	0.907*(0.975)*	0.72*(0.95)*	0.18*(1)*	0.99*(0.95)*	0.17*(0.95)*	P<0.0001
E. singularis	0.799*(0.875)*	0.73*(0.65)*	0.72*(0.82)*	0.76*(0.53)*	0.48*(0.35)*	P<0.0001
L. sarmentosa	0.907*(0.802)*	0.66*(0.66)*	0.34*(0.29)*	0.93*(0.88)*	0.27*(0.17)*	P<0.0001